ThermomiR-377-3p-induced Suppression of Cirbp Expression Is Required for Effective Elimination of Cancer Cells and Cancer Stem-like Cells by Hyperthermia

Tao-Yan Lin
Cancer Research Institute, Southern Medical University School of Basic Medical Sciences
Jun-Shuang Jia
Cancer Research Institute, Southern Medical University School of Basic Medical Sciences
Wei-Ren Luo
Department of Pathology, The Second Affiliated Hospital of Southern University of Science and Technology
Sheng-Jun Xiao
Department of Pathology, The Second Affiliated Hospital, Guilin Medical University
Xiao-Lin Lin
Cancer Research Institute, Southern Medical University School of Basic Medical Sciences
Jie Yang
Central Hospital: Hopital Central
Jia-Wei Xia
The Third People's Hospital of Kunming
Chen Zhou
Department of Pathology, The Second Affiliated Hospital, Guilin Medical University
Zhi-Hao Zhou
Cancer Research Institute, Southern Medical University School of Basic Medical Sciences
Shu-Jun Lin
Cancer Research Institute, Southern Medical University School of Basic Medical Sciences
Qi-Wen Li
Cancer Research Institute, Southern Medical University School of Basic Medical Sciences
Hong-Fen Shen
Cancer Research Institute, Southern Medical University School of Basic Medical Sciences
Yei Le
Laboratory Animal Center, Southern Medical University
Zhi-Zhi Yang
Cancer Research Institute, Southern Medical University School of Basic Medical Sciences
Wen-Qing Yang

Shool of Laboratory Medicine and Biotechnology, Southern Medical University

Lin-Bei Chen

Shool of Laboratory Medicine and Biotechnology, Southern Medical University

Shu-Wen Xue

Cancer Research Institute, Southern Medical University School of Basic Medical Sciences

Yong-Long Li

Laboratory Animal Center, Southern Medical University

Fang Wei

Cancer Research Institute, Southern Medical University School of Basic Medical Sciences

Rong Xiao-Xiang

Southern Medical University Nanfang Hospital Department of Oncology

Xiao-Jun Luo

Cancer Center, Integrated Hospital Taditional Chinese Medicine, Southern Medical University

Bing-Xia Zhao

Cancer Research Institute, Southern Medical University School of Basic Medical Sciences

Wen-Hua Huang

National Key Discipline of Human Anatomy, Southern Medical University School of Basic Medical Sciences

Yan Sun

Zhongshan shool of Medicine, Sun Yet-sun University

Dong Xiao (Xiao_d@hotmail.com)

Cancer Research Institute, Southern Medical University School of Basic Medical Sciences

---

Research Article

Keywords: Hyperthermia, Nasopharyngeal carcinoma (NPC), Cold-inducible RNA-binding protein (Cirbp), Temperature-sensitive miRNA-377–3p (termed thermomiR-377–3p), Cancer stem cells, Chemotherapy, Radiotherapy, Therapy resistance, DNA damage, Apoptosis, Thermosensitivity, Near-infrared (NIR) laser

Posted Date: September 28th, 2021

DOI: https://doi.org/10.21203/rs.3.rs-917435/v1

Abstract

In recent years, the development of adjunctive therapeutic hyperthermia for cancer therapy has received considerable attention. However, the mechanisms underlying hyperthermia resistance are still poorly understood. In this study, we investigated the roles of cold-inducible RNA binding protein (Cirbp) in regulating hyperthermia resistance and underlying mechanisms in nasopharyngeal carcinoma (NPC). Our results firstly revealed that hyperthermia significantly attenuated the stemness property of NPC cells, while combination treatment of hyperthermia and oridonin dramatically increased the killing effect on NPC cells and cancer stem cell (CSC)-like population. Moreover, hyperthermia substantially improved the sensitivity of radiation-resistant NPC cells and CSC-like cells to radiotherapy. Hyperthermia noticeably suppressed Cirbp expression in NPC cells and xenograft tumor tissues. Furthermore, Cirbp inhibition remarkably boosted anti-tumor-killing activity of hyperthermia against NPC cells and CSC-like cells, whereas ectopic expression of Cirbp compromised tumor-killing effect of hyperthermia on these cells, indicating that Cirbp overexpression induces hyperthermia resistance. ThermomiR-377–3p improved the sensitivity of NPC cells and cancer stem-like cells to hyperthermia in vitro by directly suppressing Cirbp expression. More importantly, our results displayed the significantly boosted sensitization of tumor xenografts to hyperthermia by Cirbp silencing in vivo, but ectopic expression of Cirbp nearly completely counteracted hyperthermia-mediated tumor cell-killing effect against tumor xenografts in vivo. Mechanistically, Cirbp silencing-induced inhibition of DNA damage repair by inactivating ATM-Chk2 and ATR-Chk1 pathways, decrease in stemness and increase in cell death contributed to hyperthermic sensitization; conversely, Cirbp overexpression-induced promotion of DNA damage repair, increase in stemness and decrease in cell apoptosis contributed to hyperthermia resistance. Taken together, these findings reveal a previously unrecognized role for Cirbp in positively regulating hyperthermia resistance and suggest that thermomiR-377–3p and its target gene Cirbp represent promising targets for therapeutic hyperthermia.

Background

In recent years, the development of therapeutic hyperthermia for cancer therapy has received considerable attention [1-4]. Therapeutic hyperthermia is a therapeutic procedure that increases the temperature of tumor-loaded tissues to 40-43°C, while the biological rationale for hyperthermia therapy is based on a direct cell-killing effect at a heat-shock temperature above 41–42°C[1-4]. Because of its advantages of non-toxic side effects, no damage to human normal tissues, no damage to their own immunity and so on, hyperthermia therapy has become the fifth method of cancer therapy after surgery, chemotherapy, radiotherapy and immunotherapy, and plays an important role in multidiscipline therapy for various cancers[1-4]. In recent years, a large number of in vitro and in vivo experiments and clinical data demonstrate that as an adjunctive therapy, hyperthermia combined with radiotherapy and-/or chemotherapy improves clinical outcome in cancer therapy[1-4]. More importantly, in recent years, the development of nanotechnology-based hyperthermia therapy [i.e., Nano-Photo-Thermal Therapy (NPTT), Nano-Magnetic Hyperthermia (NMH) and Nano-Ultrasound Hyperthermia (NUH)] for cancer therapy is a

growing area of cancer nanomedicine because of the potential for localized and targeted destruction of cancer cells, and great breakthroughs in nanotechnology for cancer thermotherapy have been already attained[3, 5-10].

Even though therapeutic hyperthermia is a promising adjunctive therapy for cancer, a number of obstacles remain to be cleared [1-10]. One of the major issues is that the molecular mechanisms involved in tumor response to thermal therapy are largely undefined. At present, there are several lines of evidence showing the underlying mechanisms of tumor response to hyperthermia[11-14]. A previous study showed that inhibition of telomerase activity enhanced hyperthermia-mediated radiosensitization[11]. Hyperthermia sensitized glioma stem-like cells to radiation by pharmacologically inhibiting AKT signaling[12]. CTGF silencing sensitized resistant cells to hyperthermia in vitro and in vivo[13]. Hyperthermia synergized with chemotherapy by inhibiting PARP1-dependent DNA replication arrest[14]. However, great endeavors will still be needed to fully dissect the molecular mechanisms involved in tumor response to hyperthermia, especially involved in hyperthermia resistance, which is critical to manipulate key pathways to greatly improve the clinical efficacy of hyperthermia.

Cold-inducible RNA binding protein (Cirbp, also known as A18 hnRNP or CIRP), a member of cold shock protein family and a stress-inducible protein, is activated by various cellular stresses, such as heat- and cold-treatment, hypoxia and UV-irradiation[15-21]. Accumulated evidence reveals that Cirbp has been implicated in different physiological and pathological processes, including cell proliferation and differentiation, cell senescence, cell survival and apoptosis, oxidative stress, DNA damage and repair, immune and inflammatory responses, telomere maintenance, circadian rhythm, spermatogenesis, and tumor formation and progression, etc[15-17, 19-23]. Of note, several lines of evidence has indicated that Cirbp is associated with cell stresses, including heat and cold[24-29]. Chronic hypoxia-induced Cirbp hypermethylation attenuated hypothermic cardioprotection via down-regulation of ubiquinone biosynthesis[24]. Therapeutic hypothermia protected photoreceptors through activating Cirbp pathway[25]. The down-regulation of Cirbp expression was observed in male germ cells of mice and humans under heat stress condition[26-28]. Moreover, in prostate cancer cells, heat treatment upregulated heart shock proteins and down-regulated cold shock proteins [i.e., Cirbp and RNA binding motif protein 3 (RBM3)][29]. Taken together, the aforementioned findings indicate that Cirbp might play an important role during hyperthermia treatment for cancer therapy. In this context, however, more direct evidence is needed, and the biological mechanisms remain to be understood, for clarification and characterization of the importance of Cirbp in thermotherapy for cancer treatment.

Human nasopharyngeal carcinoma (NPC) is one of the most common malignant tumors in East and Southeast Asia[30-32]. At present, the standard therapy for patients with locoregionally advanced NPC is radiation therapy combined with chemotherapy[30-32]. Furthermore, with the widespread use of intensity-modulated radiation therapy and combined radiochemotherapy, locoregional control has improved substantially, whereas distant metastasis and local recurrence are now the main cause for treatment failure in local advanced NPC[30-32]. Novel and effective adjuvant therapy (e.g., hyperthermia) for NPC is urgently warranted. In the field of NPC, a small amount of clinical trials preliminarily demonstrated that

hyperthermia combined with radiation therapy improved progression-free survival and local progression-free survival of NPC patients, although no increase in overall survival was observed[33-36]. However, in contrast to other solid cancers[1-10], the development of effective hyperthermia treatment for NPC didn't receive considerable attention. Therefore, intensive research work will still be required to develop effective hyperthermia treatment for NPC.

Against this background, in this study, we fully investigated the direct cell-killing activity of hyperthermia alone or combined treated with chemotherapy or radiotherapy on cancer cells and stem-like cancer cells of NPC. On the other hand, we clarified the potential functions of Cirbp in thermotherapy for NPC treatment in vitro and in vivo, and the molecular mechanisms underlying thermoresistance and thermosensitization.

Materials And Methods

Cell culture

Human NPC cell lines (i.e., CNE2, SUNE1 and HONE1-EBV cells) were obtained from Prof. Qiao Tao (Chinese University of Hong Kong, Hong Kong, China), Prof. S.-W. Tsao (University of Hong Kong), Prof. Yixin Zeng (Sun Yat-sen University, Guangzhou, China) and Prof. Musheng Zeng (Sun Yat-sen University, Guangzhou, China). These NPC cell lines were cultured in RPMI 1640 medium supplemented with 10% fetal bovine serum (FBS; Biological Industries) in a humidified incubator with 5% CO_2 at 37°C. Human HCC cell lines, including SMMC-7721 and Huh-7 cells, were purchased from the Type Culture Collection of the Chinese Academy of Sciences, Shanghai, China. SMMC-7721, Huh-7 and HEK293T cells were maintained in DMEM medium supplemented with 10% FBS in a humidified incubator with 5% CO_2 at 37°C.

Development of radioresistant subclone CNE2-8G cells

To obtain radiation-resistant NPC cell line, CNE2 cells were exposed to repeated X-ray irradiation, and after a total dose of 8Gy in 8 fractions, a radioresistant monoclone CNE2-8G was obtained.

RNA isolation, reverse transcription and quantitative real-time PCR (qRT-PCR)

RNA isolation, reverse transcription and qRT-PCR were well described previously[17, 37-46]. The primers used in the qRT-PCR assay are listed in Table S1. GAPDH or U6 snRNA was used as an endogenous control. All samples were normalized to internal controls, and fold changes were calculated through relative quantification ($2^{-\triangle\triangle Ct}$).

Western blotting assay

Western blotting was performed according to previous publications[39, 40, 43-48].
The primary antibodies used for Western blot were listed in Table S2. GAPDH was used as a loading control.

CCK-8 assay, colony formation assay, EdU assay, tumor sphere formation assay and apoptosis assay

Tumor-killing activity of hyperthermia, oridonin (Ori) and IR against cancer cells were assessed by Cell Counting Kit-8 (CCK-8) assay, colony formation assay and tumor sphere formation assay. Before performing the aforementioned assays, cancer cells were firstly sham-treated and treated with hyperthermia (at 42°C or 44°C for 30min), treated with Ori (concentration: 0, 20, 40, 60, 80, 100, 120, 140 and 160mM), treated with hyperthermia (42°C for 30min) and Ori (20mM Ori for 30min) alone or combined, and treated with hyperthermia (42°C for 30min) and IR (4Gy) alone or combined. Subsequently, these treated cells were further employed in the above-mentioned assays. CCK-8 assay (Dojindo, Japan), colony formation assay, EdU assay and tumor sphere formation assay were performed as previously described[39, 41, 45, 46, 49, 50].

For the CCK-8 assay, the indicated cells were plated in 96-well plates at 1×10^3 per well in a final volume of 200 μl and then cultured for 6 days. For the colony formation assay, cells were counted and plated at $1x10^3$ per well in 6-well plates for 14 days. For tumor sphere formation assay, NPC cells ($1x10^3$/well) were grown in serum-free DMEM-F12 supplemented with 10 μg/L bFGF, 20 μg/L EGF and 2% B27 in ultra-low adhesion plates (Corning, USA). Two weeks later, spheres larger than 100μm were counted by an inverted microscope (Nikon Eclipse Ti-U), and images were acquired. For the EdU assay, the proliferating NPC cells were examined using the Cell-Light EdU Apollo 567 In Vitro Imaging Kit (RiboBio) according to the manufacturer's protocol.

For the apoptosis assay, cell apoptosis rate was determined by flow cytometry with the Annexin V-APC/7-AAD Apoptosis Kit (Keygen, Jiangsu, China) according to the manufacturer's protocol. Cells were collected, stained with Annexin V and PI for 15min in the dark, and then analyzed by a FACS Caliber flow cytometer (BD Bioscience).

Percentages of side population cells (SP cells) analyzed by flow cytometry

NPC cells treated with hyperthermia (at 42°C or 44°C for 30min) were digested with 0.25% trypsin, washed twice with calcium/magnesium-free PBS, resuspended in ice-cold RPMI-1640 medium (supplemented with 2% FBS) at a concentration of 1×10^6 cells/mL, and incubated at 37°C in a 5% CO_2 incubator for 90min. Following this, the changes in the percentage of SP cells were analyzed by flow cytometry (BD FACSAria).

Plasmids, lentivirus production and transduction

The fragment (519 bp) of Cirbp was amplified from pENTER-Cirbp [purchased from Vigene Biosciences Co., Ltd. (Jinang, Shandong, China)], and then directly inserted into *Eco*R I and *Bam*H I sites of the lentivirus vector of pCDH-EF1-MCS-GFP-Puro (pLV-con as empty vector) [Cat. # CD550A-1; purchased from System Biosciences (SBI)] to generate pCDH-EF1-Cirbp-GFP-Puro (i.e., pLV-Cirbp). All lentivirus-mediated RNAi knockdown plasmids of Cirbp [purchased from Vigene Biosciences Co., Ltd. (Jinang,

Shandong, China)] were constructed in a modified pLKO.1-puro vector. The shRNA sequences against Cirbp were presented in Table S2.

For miR-377 overexpression, a fragment containing the precursor sequence of human miR-377 was cloned into the Lentivirus vector of pEZX-MR02, designated pLV-miR-377 [purchased from GeneCopoeia, Inc. (Guangzhou, China)].

The lentiviral packaging plasmids psPAX2 and pMD2.G were kindly provided by Prof. Didier Trono (University of Geneva, Geneva, Switzerland). To generate stable cell lines, recombinant lentiviruses [named as LV-shSCR (SCR: scrambled control shRNA) and LV-con (used as control), and LV-shCirbp, LV-Cirbp and LV-miR-377] were generated as previously described[41, 45, 46, 49], and subsequently used to infect the indicated cells (i.e., CNE2, SUNE1 and HONE1-EBV cells) to generate shSCR-, vector-, shCirbp-, Cirbp- or miR-377-expressing cancer cell lines, respectively.

miRNAs transient transfection

Mimics-NC, mimics, inhibitors-NC and inhibitors of miR-377-3p and miR-381-3p were purchased from RiboBio (Guangzhou, China). Transient transfection was carried out using Lipofectamine 2000 (Thermo Fisher Scientific, Waltham, MA) according to the manufacturer's recommendation.

Luciferase reporter assay

The dual luciferase reporter gene plasmid (i.e., pLuc-Cirbp-3'-UTR-wt) containing the putative miR-377 binding site at the 3'-UTR of Cirbp mRNA and the corresponding pLuc-Cirbp-3'-UTR-mut were purchased from Kangbio(Shenzhen, China). Cells were seeded in 48-well plates and cultured for 48 hours. The pLuc-Cirbp–3'-UTR-wt or pLuc-Cirbp-3'-UTR-mut was co-transfected into HEK293T cells with the miR-377-3p mimics, mimics control, miR-377-3p inhibitor or inhibitor control using Lipofectamine 2000 Reagent (Invitrogen), respectively. Luciferase and Renilla activities were assayed 48 hours after transfection using the Dual Luciferase Reporter Assay Kit (Promega) following the manufacturer's instructions.

Immunofluorescent (IF) staining

IF staining was performed according to the protocol of a standard method described previously[39, 51]. The slides were counterstained with DAPI (Sigma) for 5min to visualize the nuclei and imaged with a confocal laser-scanning microscope (Nikon A1). The primary antibodies used for IF staining were listed in Table S2.

NPC cells grown on coverslips were rinsed with PBS, and then fixed with cold 4% paraformaldehyde for 5min at room temperature. Subsequently, the cells were permeabilized with 0.3% Triton X-100 for 30min, and then incubated with primary monoclonal antibodies 53BP1 (Cat. No. ab175933, 1:250, Abcam) and γ-H2AX (Cat. No. ab26350, 1:500, Abcam) for 2h at room temperature, respectively. After three washes in PBS for 5min each, the slides were incubated for 1h in the dark room with goat anti-rabbit IgG (H+L) Dylight 549 and goat anti-Mouse IgG (H+L) Dylight 549 (1:1000, Bioworld Technology, Inc.),

respectively. Finally, the slides were counterstained with DAPI (Sigma) for 5min to visualize the nuclei and imaged with a confocal laser-scanning microscope (Nikon A1). The primary antibodies used for IF staining were listed in Table S2.

RNA sequencing

Total RNAs were extracted from Cirbp-expressing and shCirbp-expressing NPC cells treated without or with hyperthermia at 42°C for 30min using TRIzol Reagent (Invitrogen, cat. NO 15596026 following the methods by Chomczynski et al[52]. DNA digestion was carried out after RNA extraction by DNaseI. RNA quality was determined by examining A260/A280 with Nanodrop™ One spectrophotometer (Thermo Fisher Scientific Inc). RNA Integrity was confirmed by 1.5% agarose gel electrophoresis. Qualified RNAs were finally quantified by Qubit3.0 with Qubit™ RNA Broad Range Assay kit (Life Technologies, Q10210). 2 μg total RNAs were used for stranded RNA sequencing library preparation using KC-Digital™ Stranded mRNA Library Prep Kit for Illumina (Catalog NO. DR08502, Wuhan Seqhealth Co., Ltd. China) following the manufacturer's instruction. The kit eliminates duplication bias in PCR and sequencing steps, by using unique molecular identifier (UMI) of 8 random bases to label the pre-amplified cDNA molecules. The library products corresponding to 200-500 bps were enriched, quantified and finally sequenced on Novaseq 6000 sequencer (Illumina) with PE150 model.

Animal procedures and treatments

The animal experiments were carried out in strict accordance with the recommendations in the Guide for the Care and Use of Laboratory Animals of the Southern Medical University. The animal protocol was approved by the Committee on Ethics of Animal Experiments of the Southern Medical University. All surgery was performed under sodium pentobarbital anesthesia, and all efforts were made to minimize suffering of animals.

BALB/c nude mice aged 4 to 5 weeks were purchased from the Medical Laboratory Animal Center of Guangdong Province. shSCR- and shCirbp-expressing NPC cells (2×10^6), or vector- and Cirbp-expressing NPC cells (2×10^6) were subcutaneously injected into the hind limb of each nude mouse, respectively. Tumors were allowed to grow until they reached 6 to 9mm in maximal diameter, at which time the mice were randomly divided into control group (LV-shSCR and LV-shCirbp) and treatment group (LV-SCR and LV-shCirbp, ICG-NIR therapy), and into control group (LV-con and LV-Cirbp) and treatment group (LV-con and LV-Cirbp, ICG-NIR therapy). Subsequently, in treatment groups, 30min prior to laser irradiation, a single dose of 4 mg/kg of sterile ICG solution was infused by tail vein injection into each nude mouse with tumor burden, followed by a near-infrared (NIR) laser treatment (808 nm, $1w/cm^2$) for 10min. NIR laser system (Shanghai Xilong Optoelectronics Technology Co. Ltd, China) emitting 808 nm light was used in this study[53]. The laser beam diameter is 8mm, the pulse time is 3ms and the laser radiant exposure was $2W/cm^2$. In treatment group, nude mice with tumor burdens were treated by NIR laser irradiation (at 41°C~43°C) for 10min every 2 days. No treatment was applied to the mice in two control groups. A single dose of 4mg/kg of ICG solution was injected into tail vein of each mouse in

study groups. Tumor size was measured with a Vernier caliper every 2 days. Tumor volumes were calculated using the formula $a^2*b/2$, where a and b are the shorter and longer diameters of the tumor, respectively. 27 days after cancer cell implantation, mice were sacrificed, and tumor xenografts were dissected, weighed and fixed overnight in 4% paraformaldehyde, dehydrated, paraffin-embedded, sectioned, followed by H&E staining.

Statistical analysis

Data were presented as mean±SD. Statistical analyses were performed using the SPSS 20.0 software package and Graphpad 5.0 software. Two-tailed Student's t test was used for comparisons of two independent groups. The One-Way ANOVA is used for compare comparisons of multiple groups. Values are statistically significant at $^*P<0.05$, $^{**}P<0.01$ and $^{\#}P<0.001$. NS: not significant.

Results

1. Hyperthermia dramatically attenuated the stemness property of NPC and HCC cells

Hyperthermia is the use of elevated temperature for cancer treatment, in this case, typically using temperatures in the range of 41°C to 45°C. However, the suitable heat-treating temperature and time for the treatment of NPC cells is unclear. Firstly, we wanted to determine the suitable heat-treating temperature and time for the treatment of NPC cells, and the sensitivity of NPC cells (i.e., CNE2, SUNE1 and HONE1-EBV) to hyperthermia. Colony formation assay showed that the suitable heat-treating temperature and time for NPC cell treatment are 42°C and 30min, respectively (Figure S1, Figure S2 and Figure 1B). To examine the anti-tumor activity of hyperthermia treatment, we firstly evaluated the ability of hyperthermia to kill NPC cells (i.e., CNE2, SUNE1 and HONE1-EBV cells) in vitro by using CCK-8 assay. As expected, CCK-8 assay demonstrated that indicated NPC cells treated with hyperthermia at 42°C or 44°C for 30min displayed dramatically decreased cell viability, compared to control group (at 37°C) (Figure 1A). Colony formation assay illustrated that heat-treated CNE2, SUNE1 and HONE1-EBV cells (at 42°C or 44°C) demonstrated a significantly decreased colony forming ability (Figure 1B and Figure S2), compared to no hyperthermia treatment (at 37°C), while NPC cells treated with hyperthermia at 44°C exhibited a notablly reduced colony forming ability (Figure 1B and Figure S2), compared with hyperthermia treatment (at 42°C). CNE2 cells in vitro treated with hyperthermia at 42°C or 44°C for 30min displayed a significantly decreased ability of subcutaneous tumor formation in nude mice (Figure 1I,J,K and Figure S3). In addition, colony formation assay (Figure S4A) and CCK-8 assay (Figure S4B) illustrated a strong in vitro killing activity of hyperthermia therapy (at 42°C or 44°C) against hepatocellular carcinoma (HCC) cells (i.e., 7721 and Huh7 cells). Summarily, these data suggest that thermotherapy has a strong cancer cell killing activity (CKA) in vitro against NPC and HCC cells.

Since our results demonstrated that hyperthermia showed a strong CKA in vitro against NPC cells (Figure 1A,B and Figure S2), we further explored the effects of thermotherapy treatment on stem cell-like populations within NPC cells by detecting stemness markers, SP cell (side population cell) detecting

assay and tumorsphere formation assay. Heat treatment (at 42°C) in the indicated NPC cells resulted in the remarkable downregulation of stem cell-related markers (i.e., ABCG2, Bmi-1, Nanog and Sox2) at mRNA (Figure 1C) and protein (Figure 1D) levels. Furthermore, SP cells within NPC cells and tumorspheres have been reported to exhibit the characteristics of cancer stem cells (CSCs)[39, 50, 54-57]. We examined the effects of hyperthermia treatment on the percentages of SP cells within NPC cells, and observed that hyperthermia dramatically decreased the percentages of SP cells in CNE2 [1.5% (at 42°C) or 0.7% (at 44°C) vs. 2.2% (at 37°C)], SUNE1 [3.3% (at 42°C) or 3.0% (at 44°C) vs. 3.9% (at 37°C)] and HONE1-EBV cells [1.6% (at 42°C) or 0.2% (at 44°C) vs. 3.2% (at 37°C)](Figure 1E,F). This data was confirmed on several occasions, and found to be statistically significant (Figure 1F). Subsequently, we further examined the ability of heat-treated NPC cells to form tumor spheres. Tumorsphere formation assay indicated that hyperthermia-treated NPC cells (at 42°C or 44°C) demonstrated a dramatical decrease in tumorsphere formation efficiency (Figure 1G,H). Moreover, hyperthermia also effectively eliminated CSC-like population within HCC cells (i.e., 7721 and Huh7 cells) in vitro, as shown by detecting stemness markers (Figure S4C), detecting the percentage of $CD133^+$ cells (Figure S4D) and tumorsphere formation assay (Figure S4E). Together, our results indicate that hyperthermia treatment can efficiently kill cancer stem-like cell populations within NPC and HCC cells.

2. Combination treatment of hyperthermia and oridonin significantly increased the killing effect on NPC cells and stem-like cancer cells

Natural product oridonin (Ori) and its analogue alone or combined with chemotherapy and radiotherapy were reported to effectively kill tumor cells of leukemia, ovarian cancer, lung cancer, esophageal squamous cell carcinoma, osteosarcoma, breast cancer, colorectal cancer and prostate cancer[58-72]. To explore whether combination treatment of hyperthermia and Ori could significantly enhance the cell-killing effect on NPC cells and stem-like cancer cells, we first evaluated the effects of the different concentrations of Ori on cell viability. As shown in Figure 2A, the results from CCK-8 assay revealed that high concentrations of Ori markedly reduced cell viability of CNE2 and SUNE1 cells. Subsequently, we further examined the effects of Ori treatment on the stemness maintenance ability of NPC cells by detecting stemness genes and tumorsphere formation assay. qRT-PCR showed that Ori treatment (20, 40 and 60mM) led to the significantly reduced expression of stem cell-related markers (i.e., ABCG2, Bmi-1, Nanog and Sox2) in NPC cells (Figure 2B). Sphere-forming assay illustrated that Ori-treated CNE2 and SUNE1 cells demonstrated a dramatical decrease in tumorsphere formation efficiency in a dose-dependent manner (Figure 2C,D). Collectively, this work is first to reveal that Ori treatment effectively eliminates CSC-like population within NPC cells.

Next, we further determined whether combination treatment of hyperthermia and Ori significantly enhanced the antitumor cell-killing effects on NPC cells and stem-like cancer cells by CCK-8 assay, colony formation assay and tumorsphere formation assay. Our results showed that combination treatment of hyperthermia and Ori in CNE2 and SUNE1 cells significantly reduced cell viability (Figure 2E), colony forming ability (Figure 2F,G) and tumorsphere formation ability(Figure 2H,I), compared with hyperthermia

or Ori alone. Collectively, the combination treatment of hyperthermia and Ori dramatically increases the antitumor cell-killing effect against NPC cells and CSC-like population.

3. Development of radiation-resistant NPC cell line CNE2-8G

The resistance of cancer cells to radiotherapy (RT) is a major obstacle in the clinical treatment of head and neck cancer (HNC), including NPC. As RT is regarded as the mainstay treatment for patients with NPC, we intended to determine whether hyperthermia could significantly boost the anti-tumor effect of RT against radiation-resistant NPC cells and cancer stem-like cells. To that end, we firstly developed the radioresistant NPC cell line according to the experimental procedure described in the section of Materials and Methods. After CNE2 cells were exposed to repeated X-ray irradiation with a total dose of 8Gy in 8 fractions, we observed that RT-treated CNE2 cells (designated CNE2-8G cells) underwent the morphological transition from a cuboidal epithelial-like to an elongated mesenchymal-like phenotype (Figure 3A), indicating the induction of epithelial-mesenchymal transition (EMT) in CNE2-8G cells. This prompted us to characterize the existence of EMT in CNE2-8G cells at the molecular level. Western blot analysis illustrated that spindle-like and fibroblastic morphological conversion was accompanied by the increased expression of mesenchymal markers (i.e., vimentin and N-cadherin) and the reduced expression of epithelial markers (i.e., E-cadherin and b-catenin) in CNE2-8G cells (Figure 3B). Therefore, these results suggest that CNE2-8G cells display mesenchymal-like morphological change and EMT-like cellular marker alterations.

The previous studies showed that cancer cells (including NPC cells) that undergo EMT have been shown to acquire increased stemness [7, 55, 73-77]. In this study, we found that CNE2-8G cells undergoing EMT-like phenotype changes displayed the upregulated expression of stem cell-related genes (i.e., ABCG2, Nanog and Sox2) at protein levels (Figure 3B), a significantly elevated cell viability (Figure 3C) and a dramatical increase in tumorsphere formation ability (Figure 3D,E), compared with control cells (i.e., parental CNE2 cells), suggesting that CNE2-8G cells exhibit an increased stemness. Moreover, CCK-8 assay indicated that compared with CNE2 cells, CNE2-8G cells displayed an obviously elevated cell proliferation capacity even in the absence of ionizing radiation (IR)(Figure 3C).

It is well known that CSCs have been identified as the main center of therapeutic resistance of cancer cells to conventional radiotherapy, chemotherapy, immunotherapy and thermal therapy[7, 73-76, 78-81]. Additionally, IR is known to induce CSC properties[74]. Considering the significantly enhanced CSC-like populations within CNE2-8G cells, we further determined the resistance of CNE2-8G cells to RT by CCK-8 assay (Figure 3F), colony formation assay (Figure 3G) and tumorsphere formation assay (Figure 3H). The survival curves of CNE2-8G cells and CNE2 cells detected by CCK-8 assay suggested that the viability of CNE2-8G cells was significantly higher than that of CNE2 cells before and after IR (4 and 8Gy)(Figure 3F), indicating that the established CNE2-8G subclone cells are more radiation-resistant than the parental CNE2 cells. Moreover, IR with 4Gy had no statistically significant effect on colony formation (P=0.0856) (Figure 3G) and tumorsphere formation(P=0.0708)(Figure 3H and Figure S5A) of CNE2-8G cells, as compared with CNE2-8G cells treated without IR. In contrast, IR with 4Gy noticeably attenuated colony

formation of CNE2 cells by about 80.50% (P<0.05)(Figure 3G) and tumorsphere formation of CNE2 cells by about 83.30%(P<0.05) (Figure 3H), as compared with CNE2 cells treated without IR. Furthermore, IR with 8Gy led to substantially decreased colony formation of CNE2-8G cells and CNE2 cells by about 98.00% and 99.33% (Figure 3G), respectively, and resulted in appreciably reduced tumorsphere formation ability of CNE2-8G cells and CNE2 cells by about 96.84% and 98.67% (Figure 3H), respectively, as compared with CNE2-8G cells or CNE2 cells treated without IR. Therefore, the established NPC cell line CNE2-8G shows higher radioresistance than parental cell line CNE2.

4. Hyperthermia significantly improved the sensitivity of radiation-resistant NPC cells and cancer stem-like cells to radiotherapy

Subsequently, we examined the ability of thermotherapy to improve the radiosensitivity of radiation-resistant CNE2-8G cells by CCK-8 assay (Figure 3I), colony formation assay (Figure 3J) and tumorsphere formation assay (Figure 3K), and detecting stem cell-related gene expression (Figure 3L). As shown in Figure 3I, CCK-8 assay suggested that treatment of CNE2-8G cells with combined hyperthermia and radiotherapy significantly decreased cell number compared to radiation therapy alone, and we found that thermoradiotherapy treatment showed an additive effect in reducing cell viability compared to radiation therapy alone. Radiation alone had no statistically significant effect on colony formation(P=0.076) (Figure 3J and Figure S5B) and tumorsphere formation(P=0.061)(Figure 3K and Figure S5C) of CNE2-8G cells, as compared with control cells (at 37℃). Hyperthermia alone appreciably attenuated colony formation by about 84.93% (Figure 3J and Figure S5B) and tumorsphere formation by about 63.64% (Figure 3K and Figure S5C), as compared with control cells (at 37℃). The most effective treatment is thermoradiotherapy, which substantially reduced colony formation by about 98.63% (Figure 3J and Figure S5B) and tumorsphere formation by about 95.46% (Figure 3K and Figure S5C), as compared with control cells (at 37℃). Furthermore, qRT-PCR assay revealed that thermoradiotherapy led to a dramatically decreased expression of stem cell-related genes (i.e., ABCG2, Bmi-1, Nanog and Sox2)(Figure 3L), as compared to radiotherapy or hyperthermia alone, indicating that thermoradiotherapy showed a synergistic effect on reducing stem cell-related gene expression. Together, these above-mentioned studies illustrate that hyperthermia significantly improves the sensitivity of radiation-resistant NPC cells and cancer stem-like cells to radiotherapy, while thermoradiotherapy is more effective than IR alone in substantially boosting the anti-tumor activity against NPC cells and cancer stem-like cells.

5. Hyperthermia significantly suppressed Cirbp expression in NPC cells and xenograft tumor tissues formed by NPC cells in nude mice

Next, to gain insight into the underlying mechanisms via which hyperthermia exerts its tumor-killing effect on NPC cells, we performed RNA-sequencing (RNA-seq) in NPC cells treated without and with hyperthermia at 42°C for 30min. Comparing hyperthermia-treated NPC cells to control, a total of 7510 genes with expression changes of greater than 2-fold were identified(Figure 4A, Figure S6, Table S3 and Table S4) and classified using GO categories(Figure 4B and Table S5). Gene ontology (GO) enrichment analysis of these 7510 genes showed that a handful of genes were associated with cellular response to

heat, DNA damage and repair, cell cycle and cell death in cancer cells treated with hyperthermia (Figure 4B and Table S5). Figure 4A indicated that the expression of a great number of the member of heat shock protein family, such as HSP90AA1, HSP90AA2P, HSP90AA4P, HSP90AB1, HSP90B1, HSPA13, HSPA4, HSPA4L, HSPA8, HSPA9P1, HSPB11, HSPD1, HSPD1P1, HSPE1, HSPE1-MOB4 and HSPE1P2, was significantly up-regulated in hyperthermia-treated NPC cells, while the decreased expression of Cirbp (Cold inducible RNA binding protein) was observed in heat-treated cells. It is well known that the cold shock proteins (CSPs), namely Cirbp and RNA binding motif protein 3 (RBM3) are induced upon hypothermia and other forms of cellular stress such as UV radiation and hypoxia[16, 19, 20, 29, 82]. Cirbp expression was down-regulated at elevated temperature in male germ cells of mice and humans[28, 61]. The previous study indicated that Rbm3 expression was reduced during fever/pyrexia, and reduced Rbm3 expression in turn led to elevated expression of Rbm3-targeted temperature-sensitive miRNAs (termed thermomiRs), such as miR-142-5p and miR-143[83]. Moreover, cytoprotective Rbm3 expression was induced by cooling but suppressed by pyrexia in cardiomyocytes[84]. Together, these aforementioned findings strongly suggests that Cirbp and Rbm3 might be implicated in hyperthermia for cancer therapy.

Considering the potentially important roles of Cirbp and Rbm3 in hyperthermia for cancer therapy, we first examined the effects of hyperthermia treatment on the expression of thermomiRs (i.e., miR-142-5p and miR-143)(used as positive control)[83], and Cirbp and Rbm3 by qRT-PCR. NPC cells (i.e., CNE2, SUNE1 and HONE1-EBV) were treated by heating at 42°C for 30min. As shown in Figure 4C, the results from qRT-PCR assay revealed that miR-142-3p and miR-143 were significantly upregulated, and Cirbp was remarkably downregulated in hyperthermia-treated NPC cells (i.e., CNE2, SUNE1 and HONE1-EBV). In contrast, there was no significant change in Rbm3 expression in hyperthermia-treated NPC cells (Figure 4C). In keeping with these aforementioned findings (Figure 4C), Western blot analysis also showed the dramatically downregulated protein expression of Cirbp in heating-treated CNE2, SUNE1 and HONE1-EBV cells (Figure 4D). To further validate these mentioned-above observations in vitro, we expanded our investigation into heating-treated xenograft tumor tissues. We found that hyperthermia notably suppressed Cirbp protein expression in heating-treated xenograft tumor tissues formed by CNE2 cells in nude mice (Figure 7I and Figure 8I). Collectively, our data demonstrate that hyperthermia treatment appreciably inhibits Cirbp expression in NPC cells and xenograft tumor tissues, which led us to reasonably speculate that Cirbp silencing might induce the sensitization of NPC cells and cancer stem-like cells to hyperthermia.

6. Cirbp suppression by RNAi significantly improved the sensitivity of NPC cells and cancer stem-like cells to hyperthermia in vitro

To test above-mentioned hypothesis, we first evaluated the effects of Cirbp silencing by RNAi (Figure S7) on the sensitivity of NPC cells and cancer stem-like cells to hyperthermia in vitro by CCK-8 assay (Figure 4E and Figure S8A), colony formation assay (Figure 4F and Figure S8B), tumorsphere formation assay (Figure 4G and Figure S8C) and apoptosis assay (Figure 4H and Figure S8D). The Cirbp-shRNA specifically knocked down endogenous Cirbp mRNA (Figure S6B) and protein (Figure S6C) expression in

CNE2, SUNE1 and HONE1-EBV cells. Our results revealed that Cirbp knockdown led to significant cell viability inhibition (Figure 4E and Figure S8A), colony formation suppression (Figure 4F and Figure S8B) and tumorsphere formation inhibition (Figure 4G and Figure S8C), similar to those induced by hyperthermia treatment, suggesting that down-regulating Cirbp in NPC cells might mimic the stress response the cells experience when exposed to heat treatment. More importantly, treatment with combined hyperthermia and shRNA-mediated Cirbp silencing resulted in a substantial reduction in cell survival ability (Figure 4E and Figure S8A), colony formation suppression (Figure 4F and Figure S8B) and tumorsphere formation inhibition (Figure 4G and Figure S8C), as compared to thermotherapy alone. Together, these findings clearly demonstrate that Cirbp inhibition by RNAi significantly improve the thermosensitivity of NPC cells and cancer stem-like cells in vitro.

7. Cirbp overexpression counteracted the tumor-killing effect of hyperthermia on NPC cells and cancer stem-like cells in vitro

Next, we further elucidated the effects of Cirbp overexpression on the sensitization of NPC cells and cancer stem-like cells to hyperthermia in vitro by CCK-8 assay (Figure 5A), colony formation assay (Figure 5B), tumorsphere formation assay (Figure 5C) and apoptosis assay (Figure 5D). The Cirbp transgene was successfully over-expressed in CNE2, SUNE1 and HONE1-EBV cells (Figure S7). As shown in Figure 5A, CCK-8 assay revealed that the ectopic expression of Cirbp in CNE2 and SUNE1 cells had no statistically significant effect on cell viability, as compared with control cells (i.e., LV-con), while CCK-8 assay showed that exogenous expression of Cirbp in HONE1-EBV cells had a slight, but statistically significant impact on cell number, as compared with control cells (i.e., LV-con). Moreover, our results from colony formation assay(Figure 5B and Figure S10A) showed that exogenous expression of Cirbp had no statistically significant effect on CNE2 cell growth, and had a slight, but statistically significantly growth-promoting impacts on cell proliferation of SUNE1 and HONE1-EBV cells in vitro, as compared with control cells (i.e., LV-con). More importantly, both CCK-8 assay (Figure 5A) and colony formation assay (Figure 5B and Figure S10A) indicated that there was no significant difference in cell survival and cell proliferation of CNE2, SUNE1 and HONE1-EBV cells between LV-Cirbp+42℃cells and LV-Cirbp cells, suggesting that ectopic expression of Cirbp completely rescued hyperthermia-induced decrease in cell viability and cell growth in vitro.

In addition, our data from tumorsphere formation assay (Figure 5C and Figure S10B,C,D) demonstrated that the enforced expression of Cirbp had a slight, but statistically significantly growth-promoting effect on tumorsphere formation of CNE2 and SUNE1 cells, and displayed a significantly positive impacts on tumorsphere formation of HONE1-EBV cells, as compared with control cells (i.e., LV-con). More importantly, there was no statistically significant difference in tumorsphere formation efficiency of CNE2 cells between LV-Cirbp+42℃cells and LV-Cirbp cells (Figure 5C and Figure S10B). As shown in Figure 5C and Figure S10C,D, heating treatment significantly reduced tumorsphere number in Cirbp-expressing SUNE1 and HONE1-EBV cells by about 12.20% (for SUNE1 cells) and 14.58% (for HONE1-EBV cells) compared to LV-Cirbp cells, whereas LV-con+42℃cells displayed a substantial decrease in tumorsphere number by about 34.09% (for SUNE1 cells) and 67.07% (for HONE1-EBV cells), as compared

to LV-con cells. Therefore, these aforementioned results clearly suggest that re-expression of Cirbp completely or mostly rescues hyperthermia-induced reduction in tumorsphere formation efficiency, indicating that re-expression of Cirbp induces hyperthermia resistance.

8. Cirbp knockdown greatly promoted cell apoptosis and thus substantially enhanced the sensitivity of NPC cells to hyperthermia

To address whether Cirbp silencing-induced sensitization of NPC cells and cancer stem-like cells to hyperthermia in vitro is due to apoptosis, flow cytometry for the apoptosis assay was performed. In this study, we observed that hyperthermia treatment alone had little effect on apoptosis or had a slight, but statistically significant impact on apoptosis induction, compared to sham-treated cells (i.e., LV-shSCR) (Figure 4H and Figure S8D) or (i.e., LV-con)(Figure 5D and Figure S10E). Moreover, Cirbp overexpression had minimal effect on apoptosis compared to sham-treated cells (i.e., LV-con)(Figure 5D and Figure S10E). However, Cirbp inhibition by RNAi had pronounced apoptosis-promoting effect on CNE2, SUNE1 and HONE1-EBV cells(Figure 4H, Figure 5D, Figure S8D and Figure S10E). Furthermore, the proportion of apoptotic cells of Cirbp knockdown plus 42℃ group increased significantly compared to those of the control group (LV-shSCR), shSCR+42℃group or shCirbp group(Figure 4H and Figure S8D). Collectively, our results show that RNAi-mediated Cirbp suppression can greatly promote cell apoptosis, and thus substantially increase the sensitivity of cancer cells to hyperthermia.

To further identify genes involved in cell apoptosis and cell survival, we performed RNA-seq in shSCR- and shCirbp-expressing SUNE1 cells. Comparing shCirbp-expressing cells to control cells, differentially expressed genes with expression changes of greater than 2-fold were identified(Figure 4K and Table S6) and classified using GO categories (Figure 4L and Table S7) and KEGG pathway (Figure 4L and Table S8). All GO terms representing biological processes listed in Figure 4L and Table S7 were related to cell apoptosis, cell death and cell survival. Moreover, the functional classification of the differentially expressed mRNA transcripts based on KEGG pathway analysis also demonstrated that the downregulated genes in shCirbp-expressing SUNE1 cells are highly associated with PI3K-Akt signaling pathway and cGMP-PKG signaling pathway(Figure 4L and Table S8). Together, these results from GO annotation and pathway enrichment analysis of differentially expressed genes illustrate a significant enrichment for 32 genes with functions typically associated with cell apoptosis, cell death and cell survival, indicating that these altered genes involved in cell survival could be responsible, or contribute to the substantially increased sensitivity of shCirbp-expressing cancer cells to hyperthermia.

9. ThermomiR-377–3p improved the sensitivity of NPC cells and cancer stem-like cells to hyperthermia *in vitro* by directly suppressing Cirbp expression

miRNAs are being considered as potential therapeutic targets for various diseases, including hepatitis and cancers[45, 85-89], while miRNA mimics and molecules that target miRNAs (anti-miRs) have shown promise for clinical application in preclinical or clinical trials[90, 91], and miRNA-targeted therapeutics have already been tested in clinical trials. In addition, the previous study indicated that some miRNAs (i.e., miR-142-5p and miR-143) were identified to belong to temperature-sensitive miRNAs(termed thermomiRs)

[83]. Against this background, we intend to find out thermomiRs of which Cirbp might be a potential target gene. Based on bioinformatics prediction softwares (i.e., targetscan, mirdb, pictar and rna22), we predicted seven miRNAs (i.e. miR-124-3p, miR-145-5p, miR-27a-3p, miR-27b-3p, miR-300, miR-377-3p and miR-381-3p) of which Cirbp might be a potential target gene. Subsequently, qRT-PCR assay was employed to detect the expression levels of the aforementioned miRNAs in hyperthermia-treated NPC cells. qRT-PCR analysis revealed the significantly elevated expression of thermomiRs (i.e., miR-143 and miR-142-5p used as positive controls) and two selected miRNAs (i.e., miR-377-3p and miR-381-3p), and the remarkably reduced expression of Cirbp in all of three NPC cell lines (CNE2, SUNE1 and HONE1-EBV) treated with hyperthermia at both 40°C and 42°C (Figure 6A,B,C), whereas qRT-PCR assay didn't demonstrate the regular expression changes of other five miRNAs (i.e. miR-124-3p, miR-145-5p, miR-27a-3p, miR-27b-3p and miR-300) in two NPC cell lines (CNE2 and SUNE1) treated with hyperthermia at both 40°C and 42°C (Figure 6A,B), which prompted us to focus on two thermomiRs (i.e., miR-377-3p and miR-381-3p) for further study.

Our further study derived from qRT-PCR and Western blot illustrated that miR-377-3p (Figure 6D,E,F), but not miR-381-3p (Figure S12), negatively regulated Cirbp expression in all of three NPC cell lines (CNE2, SUNE1 and HONE1-EBV). Next, we further carried out luciferase reporter assay to determine whether miR-377-3p can directly target the 3'-UTR of Cirbp in NPC cells. The target sequence of Cirbp 3'-UTR (wt 3'-UTR) or the mutant sequence (mt 3'-UTR) was cloned into a luciferase reporter vector (Figure 6G). HEK293T cells were then transfected with wt or mt 3'-UTR vector and miR-377-3p mimics. The results showed a significant decrease of luciferase activity when compared with miR control (Figure 6H, lanes 2 and 3; $P<0.01$). The activity of mt 3'-UTR vector was unaffected by a simultaneous transfection with miR-377-3p (Figure 6H, lanes 7 and 8). Furthermore, cotransfection with anti-miR-377-3p and wt 3'-UTR vector in HEK293T led to a 2-fold increase of luciferase activity (Figure 6H, lanes 4 and 5; $P<0.001$). Together, all these results strongly suggest that Cirbp is a direct target of miR-377-3p in NPC cells.

Next, we further elucidated the effects of miR-377-3p overexpression on the sensitization of NPC cells and cancer stem-like cells to hyperthermia in vitro by colony formation assay (Figure 6I), EdU assay (Figure 6K) and tumorsphere formation assay (Figure 6J). The miR-377 transgene was successfully over-expressed in CNE2 and SUNE1 cells (Figure S13A,B). Our results revealed that miR-377-3p overexpression led to significant colony formation suppression (Figure 6I and Figure S13C), cell growth inhibition EdU assay cell viability inhibition (Figure 6K and Figure S13D) and tumorsphere formation inhibition (Figure 6J and Figure S13E), similar to those induced by hyperthermia treatment, suggesting that ectopic expression of miR-377-3p in NPC cells might mimic the stress response the cells experience when exposed to heat treatment. More importantly, treatment with combined hyperthermia and miR-377-3p overexpression resulted in a substantial reduction in colony formation suppression (Figure 6I and Figure S13C), cell growth inhibition EdU assay cell viability inhibition (Figure 6K and Figure S13D) and tumorsphere formation inhibition (Figure 6J and Figure S13E), as compared to thermotherapy alone. Together, these findings clearly demonstrate that the enforced expression of miR-377-3p significantly improve the thermosensitivity of NPC cells and cancer stem-like cells in vitro, similar to those induced by Cirbp inhibition by RNAi hyperthermia treatment.

To elucidate whether the thermosensitivity-improved effect of miR-377-3p overexpression was mediated by repression of Cirbp in NPC cells, we further evaluated whether ectopic expression of Cirbp could rescue the thermosensitivity-improved effect of miR-377-3p. To this end, exogenous expression of Cirbp was attained in miR-377-expressing NPC cells (Figure 6L). We found that ectopic expression of Cirbp significantly rescued miR-377-3p-induced colony formation suppression (Figure 6M and Figure S13F) and tumorsphere formation inhibition (Figure 6N and Figure S13G) under hyperthermia condition. Collectively, thermomiR-377–3p improves the sensitivity of NPC cells and cancer stem-like cells to hyperthermia in vitro by directly suppressing Cirbp expression.

10. Sensitization of tumor xenografts to hyperthermia by Cirbp silencing in vivo

Next, we further evaluated the in vivo effects of Cirbp suppression on the sensitization of NPC cells to hyperthermia and on tumor growth in subcutaneous xenograft tumor mouse model of NPC cells. Firstly, to this end, BALB/C nude mice were selected and the xenograft tumor models were established with NPC cell lines (i.e., CNE2, HONE1-EBV and SUNE1 cells) by subcutaneous injection, according to standard procedures described in the section of Materials and Methods. Figure 7A presents the experimental schedule for in vivo animal study. Indocyanine green (ICG) is a photothermal agent, photosensitizer, and fluorescence imaging probe which shows specific accumulation in cancer cells[92-97]. In this study, we developed a photodynamic therapy (PDT) (i.e., ICG-NIR therapy) using ICG and near-infrared (NIR) laser as an anti-tumor therapy for NPC. As showed in Figure 7A, ICG-NIR-mediated PDT was employed to further identify the in vivo effects of Cirbp inhibition on the therapeutic efficacy of thermotherapy. As indicated in Figure 7A, 30min before NIR laser treatment, we intravenously injected ICG into tumor-bearing nude mice, and subsequently we treated tumors with local hyperthermia (41°C-43°C) using an NIR laser at 808 nm for 10min. Repeated ICG-NIR irradiation with a 808 nm was carried out for 10min every 2 days. As expected, compared to control group (i.e., LV-shSCR), in vivo Cirbp suppression by RNAi in CNE2 and HONE1-EBV cell-derived xenografts resulted in a dramatical reduction in tumor size (Figure 7B,E), tumor volume (Figure 7C,F) and tumor weight (Figure 7D,G), similar to those induced by hyperthermia treatment alone (i.e., LV-shSCR+ICG)(Figure 7B-G), indicating that down-regulating Cirbp in subcutaneous tumor xenograft formed by NPC cells mimics the stress response the cells experience when exposed to local hyperthermia treatment. More importantly, the combination treatment with Cirbp silencing and local hyperthermia (i.e., LV-shCirbp+ICG) led to the dramatical inhibition of tumor growth, as shown by substantially reduced tumor size (Figure 7B,E), tumor volume (Figure 7C,F) and tumor weight (Figure 7D,G), as compared with Cirbp knockdown or hyperthermia alone. Therapeutic benefit from Cirbp inhibition plus hyperthermia combination treatment was also attained in subcutaneous xenograft model of SUNE1 cells (Figure S14A,B). Furthermore, H&E staining indicated that there were large necrotic areas within CNE2, HONE1-EBV and SUNE1 cell-derived tumor xenograft tissues in local hyperthermia alone group, similar to those induced by in vivo Cirbp suppression by RNAi (Figure 7H and Figure S14C). More importantly, the combination treatment of Cirbp silencing and local hyperthermia leads to considerablly necrotic area within xenograft tumor tissues, as compared with Cirbp inhibition or thermotherapy alone (Figure 7H and Figure S14C). Taken together, these results demonstrate that Cirbp silencing in vivo sensitizes NPC xenograft tumor to local

hyperthermia treatment, and thus substantially boosts anti-tumor killing effect of hyperthermia against NPC cells and cancer stem-like cells in vivo.

11. Exogenous expression of Cirbp counteracted the tumor-killing effect of hyperthermia against NPC cells and cancer stem-like cells in vivo

Subsequently, we further identified the in vivo effects of re-expression of Cirbp on the sensitization of NPC cells (i.e., CNE2 and SUNE1 cells) to hyperthermia and on tumor growth of NPC cell-derived xenografts (Figure 8A). As expected, in vivo local hyperthermia alone (i.e., LV-con+ICG) significantly decreased tumor size (Figure 8B,E), tumor volume (Figure 8C,F) and tumor weight (Figure 8D,G) compared to mock-treated group (i.e., LV-con). Moreover, ectopic expression of Cirbp in CNE2 (Figure 8B,C,D) and SUNE1 (Figure 8E,F,G) cells had little effect on tumor xenograft growth (Figure 8E,F,G), as compared with control cells (i.e., LV-con). More interestingly, we clearly observed there was no statistically significant difference in tumor size (Figure 8B,E), tumor volume (Figure 8C,F) and tumor weight (Figure 8D,G) of tumor xenografts formed by CNE2 or SUNE1 cells between LV-Cirbp+ICG group and LV-Cirbp group, suggesting that exogenous expression of Cirbp completely rescued hyperthermia-induced significant inhibition in tumor xenograft growth. Additionally, as expected, histological examinations after local hyperthermia treatment alone (i.e., LV-con+ICG group) revealed large necrotic areas, as compared with control group (i.e., LV-con)(Figure 8H). More interestingly, we clearly found there was no significant difference in necrotic area tumor xenograft formed by CNE2 or SUNE1 cells between LV-Cirbp+42℃group and LV-Cirbp group, suggesting that exogenous expression of Cirbp completely compromised hyperthermia-induced necrosis (Figure 8H). Taken together, our these findings evidently illustrate that ectopic expression of Cirbp completely or mostly counteracts the sensitivity of cells to hyperthermia, and thus completely or mostly neutralized the anti-tumor activity of hyperthermia against NPC cells and cancer stem-like cells in vivo, suggesting that Cirbp overexpression causes hyperthermia resistance.

12. Cirbp positively modulated the resistance of CSC-like cells to hyperthermia

CSCs are thought to be responsible for the therapeutic resistance to conventional treatments (including radiotherapy, chemotherapy, immunotherapy and thermal therapy)[7, 73-81]. Considering the importance of CSCs in the maintenance of therapeutic resistance, we further evaluated the effects of Cirbp on the sensitivity or the resistance of cancer stem-like cells to hyperthermia by tumorsphere formation assay (Figure 4G and Figure 5C) and detecting stem cell-related gene expression (Figure 5G, Figure 7J and Figure 8J). Our results revealed that Cirbp knockdown alone led to significant tumorsphere formation inhibition (Figure 4G and Figure S8C), similar to those induced by hyperthermia treatment alone, indicating that down-regulating Cirbp significantly reduces the self-renewal ability of cancer stem-like cells. More importantly, treatment with combined hyperthermia and siRNA-mediated Cirbp silencing resulted in a substantial reduction in tumorsphere formation (Figure 4G and Figure S8C), as compared to thermotherapy or LV-shCirbp group alone.

Subsequently, we further evaluated the stemness by detecting stem cell-related gene expression. Western blot analysis revealed that heat treatment (i.e., LV-con+42°C group or LV-shSCR+42°C group) or Cirbp inhibition by RNAi alone resulted in the remarkable downregulation of stem cell-related markers (i.e., Nanog, Sox2, Oct4, ABCG2 or Bmi-1) in NPC cells (i.e., CNE2, SUNE1 and HONE1-EBV cells)(Figure 5G) and in CNE2 cell-derived xenografts (Figure 7J and Figure 8J), as compared with those in control cells (i.e., LV-con group) or in control xenografts [i.e., LV-shSCR group (Figure 7J) or LV-con group (Figure 8J)], suggesting that hyperthermia or Cirbp depletion efficiently suppresses the stemness of NPC cells in vitro and in vivo. Moreover, treatment with combined hyperthermia and Cirbp silencing by RNAi dramatically reduced expression or led to almost undetectable expression levels of the indicated stem cell-related markers in whole xenograft tumor lysates from CNE2 cells (Figure 7J), as compared to those of hyperthermia or Cirbp inhibition alone. Taken together, these results indicate that Cirbp suppression-hyperthermia combination treatment efficiently attenuates the stemness property of NPC cells, which thereby contributes to significantly improving the sensitivity of cancer stem-like cells to hyperthermia.

In addition, our data from tumorsphere formation assay demonstrated that the enforced expression of Cirbp had a slight, but statistically significantly growth-promoting effect on tumorsphere formation of CNE2 and SUNE1 cells, and displayed a significantly positive impacts on tumorsphere formation of HONE1-EBV cells, as compared with control cells (i.e., LV-con)(Figure 5C and Figure S10B,C,D). More importantly, there was no statistically significant difference in tumorsphere formation efficiency of CNE2 cells between LV-Cirbp+42℃cells and LV-Cirbp cells (Figure 5C and Figure S10B,C,D). As shown in Figure 5C and Figure S10B,C,D, heating treatment significantly reduced tumorsphere number in Cirbp-expressing SUNE1 and HONE1-EBV cells by about 12.20% (for SUNE1 cells) and 14.58% (for HONE1-EBV cells) compared to LV-Cirbp cells alone, whereas LV-con+42℃cells displayed a substantial decrease in tumorsphere number by about 34.09% (for SUNE1 cells) and 67.07% (for HONE1-EBV cells), as compared to LV-con cells. These aforementioned results clearly suggest that ectopic expression of Cirbp completely or mostly rescues hyperthermia-induced reduction in tumorsphere formation efficiency.

In addition, we observed that heat treatment alone (i.e., LV-con+42°C group) led to the remarkable downregulation of stem cell-related markers (i.e., Nanog, Sox2, Oct4, ABCG2 or Bmi-1) in CNE2 cell-derived xenografts (Figure 8J), as compared with those in control xenografts [i.e., LV-con group (Figure 8J)], suggesting that hyperthermia efficiently suppresses the stemness of NPC cells in vivo. The enforced expression of Cirbp alone had little impact on the expression of stem cell-related markers (i.e., Nanog and Bmi-1) or slightly upregulated the expression of Sox2, Oct4 and ABCG2 in whole xenograft tumor lysates from CNE2 cells (Figure 8J), as compared to those of control group (i.e., LV-con group). Finally, hyperthermia led to a slight down-regulation of Nanog, Sox2, Oct4, ABCG2 or Bmi-1 in tumor xenografts formed by Cirbp-expressing CNE2 cells, as compared to those in LV-Cirbp group (Figure 8J), whereas the expression levels of Nanog, Sox2, Oct4 or ABCG2 in LV-Cirbp+42℃group were slightly higher than those in LV-con+42°C group. Thus, these data clearly suggest that ectopic expression of Cirbp partially counteracts hyperthermia-induced decrease in stem cell-related gene expression. All in all, re-expression of Cirbp completely or mostly compromises hyperthermia-induced reduction in the stemness of NPC cells, which thereby contributes to hyperthermia resistance.

13. Cirbp silencing-induced inhibition of DNA repair and increase in cell death contribute to hyperthermic sensitization

Subsequently, we intended to further investigate the underlying mechanisms by which Cirbp regulates thermosensitivity. As a stress-induced protein, Cirbp is initially described as a DNA damage-induced transcript (A18 hnRNP)[19], while Cirbp has been implicated in DNA damage and repair[15, 19, 98, 99]. Therefore, these above-mentioned findings led us to reasonably infer that Cirbp-mediated DNA damage and repair might be involved in the underlying mechanisms by which Cirbp regulates the sensitivity of cancer cells to hyperthermia.

Firstly, to further explore the impacts of Cirbp depletion on DNA damage and repair during thermotherapy, immunofluorescent staining was performed to examine the presence of DNA double-strand break (DSB) in indicated cells by assessing the formation of 53BP1(Figure 4I and Figure S9A) and γ-H2AX(Figure 4J and Figure S9B) foci. We observed that there were significantly more 53BP1-labeled CNE2, SUNE1 and HONE1-EBV cells in both LV-shSCR+42℃ group and LV-shCirbp group, as compared to those of control group (i.e., LV-shSCR)(Figure 4I and Figure S9A). Moreover, 53BP1 exhibited nuclear foci in more cancer cells of LV-shCirbp+42℃ group compared with those in LV-shSCR group, LV-shSCR+42℃ group and LV-shCirbp group (Figure 4I and Figure S9A). As shown in Figure 4J and Figure S9B, compared to that in control cells (i.e., LV-shSCR), the percentage of γ-H2AX-positive cells (i.e., CNE2 and HONE1-EBV cells) was much higher in shCirbp-expressing cells of LV-shCirbp group, similar to those induced by hyperthermia treatment alone. More importantly, our results displayed the higher percentage of γ-H2AX-positive cells in shCirbp-expressing CNE2 and HONE1-EBV cells (especially HONE1-EBV cells) that underwent thermotherapy, as compared with those in LV-shSCR group, LV-shSCR+42℃ group and LV-shCirbp group (Figure 4J and Figure S9B). Moreover, the protein levels of γ-H2AX were also quantified by Western blotting. Compared to control xenografts [i.e., LV-shSCR group (Figure 7I) or LV-con group (Figure 8I)], CNE2 cell-derived xenografts in vivo treated with hyperthermia [i.e., LV-shSCR+ICG group (Figure 7I) or LV-con+ICG group (Figure 8I)] had higher levels of γ-H2AX, while shCirbp-expressing cell-derived xenografts also showed increased levels of γ-H2AX, as compared with control xenografts [i.e., LV-con group (Figure 8I)]. Importantly, the treatment with combined hyperthermia and shCirbp showed higher level of γ-H2AX, as compared with hyperthermia or Cirbp inhibition by RNAi alone (Figure 7I). These above-mentioned findings from Western blotting (Figure 7I and Figure 8I) are consistent with the results of the immunofluorescence (Figure 4J and Figure S9B). Thus, two indicators of DSBs suggest the presence of higher incidence of DNA damage in the combination treatment group. Furthermore, as described above, shCirbp-expressing cells (i.e., CNE2, SUNE1 and HONE1-EBV cells) treated with hyperthermia exhibited higher levels of apoptosis (Figure 4H). Together, these data suggest that Cirbp silencing-induced inhibition of DNA damage repair and thus increase in cell death might contribute to hyperthermic sensitization.

Upon hyperthermia-induced DNA damage, tumor cells utilize two primarily distinct kinase signaling cascades to repair DSBs, including the ATM-Chk2 and ATR-Chk1 axes[97, 100-105]. PARP-1–dependent recruitment of Cirbp promotes double-strand break repair and genome stability[15]. Recent study reported

that Cirbp plays a crucial role in mediating the associations of MRN and ATM with chromatin[15]. Firstly, to gain more insight into the roles of hyperthermia and Cirbp knockdown alone or combined in the activation or inactivation of these DNA repair pathways, we detected the phosphorylation of ATM (p-ATM), Chk2 (p-Chk2), p53 (p-p53), ATR (p-ATR), Chk1 (p-Chk1) and BRCA1 (p-BRCA1) in shCirbp-expressing CNE2 cell-derived xenografts before and after in vivo heating treatment. Compared to control xenografts [i.e., LV-shSCR group (Figure 7I)], Cirbp knockdown alone led to the significant reduction in the phosphorylation levels of ATM (p-ATM), Chk2 (p-Chk2), p53 (p-p53), ATR (p-ATR), Chk1 (p-Chk1) and BRCA1 (p-BRCA1) in CNE2 cell-derived xenografts (Figure 7I), similar to those induced by hyperthermia treatment alone (Figure 7I and Figure 8I). As expected, treatment with combined hyperthermia and Cirbp silencing dramatically suppressed the phosphorylation levels of these above-mentioned proteins in CNE2 cell-derived xenografts compared to hyperthermia or Cirbp inhibition alone (Figure 7I). Overall, these findings indicate that Cirbp knockdown represses ATM-Chk2 and ATR-Chk1 pathways, and consequently decreases the DNA repair ability of NPC cells, ultimately enhancing thermosensitivity.

14. Ectopic expression of Cirbp induced hyperthermia resistance through promoting DNA damage repair

Secondly, we further investigated the effects of the enforced Cirbp expression on DNA damage and repair during hyperthermia using immunofluorescent staining for nuclear foci of the protein 53BP1(Figure 5E and Figure S11A) and γ-H2AX(Figure 5F and Figure S11B). We observed that hyperthermia treatment alone led to the statistically significant formation of 53BP1 (Figure 5E) and γ-H2AX (Figure 5F) foci, whereas at the absence of stress, the ectopic expression of Cirbp in the indicated cells had little effect on the formation of 53BP1 (Figure 5E and Figure S11A) and γ-H2AX (Figure 5F and Figure S11B) foci, as compared with control group (i.e., LV-con alone). More interestingly, the formation of 53BP1 (Figure 5E) and γ-H2AX (Figure 5F) foci was observed in the two groups (i.e., LV-Cirbp group and LV-Cirbp+42℃group) at virtually equal and low levels, suggesting that ectopic expression of Cirbp counteracts hyperthermia-induced formation of 53BP1 and γ-H2AX foci in LV-Cirbp+42℃group. Furthermore, there was no statistically significant difference in apoptotic cell rate between LV-Cirbp group and LV-Cirbp+42℃group (Figure 5D). Collectively, these above-mentioned findings led us to reasonably infer that Cirbp overexpression might protect cancer cells against hyperthermia-induced DNA damage, which thereby contributes to hyperthermia resistance.

To fully understand the molecular basis that contribute to the Cirbp overexpression-induced hyperthermia resistance, we performed RNA-seq in Cirbp-expressing NPC cells and Cirbp-expressing NPC cells plus 42℃. Comparing Cirbp-expressing NPC cells plus 42℃ to Cirbp-expressing NPC cells, a total of 4020 genes with expression changes of greater than 2-fold were identified(Figure 5H, Figure S15, Table S9 and Table S10) and classified using GO categories (Figure 5I and Table S11) and KEGG pathway (Figure 5I and Table S12). In the present study, we found that the biological implications of up-regulated genes in Cirbp-expressing NPC cells plus 42℃were significantly over-represented in GO biological processes related to DNA repair and cell cycle (Figure 5H,I, Table S9, Table S10 and Table S11), and KEGG pathway including p53 signaling pathway (Figure 5H,I, Table S9, Table S10 and Table S12). Cirbp that is initially described as a DNA damage-induced transcript is a stress-induced protein[19], while PARP-1-

dependent recruitment of Cirbp promotes double-strand break (DSB) repair and genome stability[15]. These above-mentioned findings from RNA-seq and published reports strongly support that ectopic expression of Cirbp activates DNA repair pathways in NPC cells under hyperthermia condition.

To gain additional insight into the effects of hyperthermia and Cirbp overexpression alone or combined on DNA damage repair pathways, we examined the changes in the aforementioned key proteins involved in the DNA repair pathways in Cirbp-expressing CNE2 cell-derived xenografts before and after in vivo heating treatment. We observed that hyperthermia treatment alone significantly reduced the phosphorylation levels of ATM (p-ATM), Chk2 (p-Chk2), p53 (p-p53), ATR (p-ATR), Chk1 (p-Chk1) and BRCA1 (p-BRCA1) in CNE2 cell-derived xenografts (Figure 8I). At the absence of stress, the ectopic expression of Cirbp in CNE2 cell-derived xenografts had little effect on the phosphorylation levels of these above-mentioned proteins involved in DNA repair pathways, as compared to those in control xenografts (i.e., LV-con group)(Figure 8I). Moreover, compared to those in LV-Cirbp group, the phosphorylation levels of ATM, Chk2, p53, ATR and Chk1 were slightly decreased in LV-Cirbp+ICG group, whereas cell-derived xenografts from LV-Cirbp+ICG group exhibited relatively higher activation of these two pathways compared to those in LV-con+ICG group (Figure 8I). These aforementioned results clearly suggests that ectopic expression of Cirbp mostly rescues hyperthermia-induced reduction in the phosphorylation levels of ATM, Chk2, p53, ATR and Chk1, which consequently reverses hyperthermia-induced reduction in DNA damage repair ability of cancer cells and increase in cell apoptosis, ultimately leading to increased thermoresistance and tumor growth (Figure 9). Summarily, these data clearly suggest that Cirbp overexpression-induced promotion of DNA damage repair and decrease in cell death contributes to hyperthermia resistance.

Discussion

As a promising adjunctive therapy, hyperthermia will play an important role in multidiscipline therapy for cancer[1-4]. However, the underlying molecular mechanisms involved in the response of tumor cells to thermal therapy still remain largely unknown. In this study, our findings uncover, for what we believe is the first time, that exogenous expression of Cirbp enhances hyperthermia resistance by promoting DNA damage repair in cancer cells, while Cirbp suppression is required for effective elimination of cancer cells and cancer stem-like cells by hyperthermia. This role of Cirbp is distinct from the established functions of Cirbp in RNA metabolism, circadian gene regulation and inflammatory response[15-17, 19-23].

Even though hyperthermia provides a promising therapeutic approach to anti-tumor therapy, huge efforts will still be required to fully examine the molecular mechanisms involved in tumor response to hyperthermia, which is critical to tremendously improve the clinical efficacy of hyperthermia by manipulating key pathways[106]. Several lines of evidence showed that the suppression of some genes or proteins, such as telomerase catalytic subunit TERT[11], AKT signaling[12], CTGF[13], HSP70[107, 108], HSP90[109] and HSP27[110] significantly boosted the effects of hyperthermia-based anti-cancer treatments. Furthermore, introduction of constitutively active AKT in glioma stem cells (GSCs) compromised hyperthermic radiosensitization[12]. Collectively, the underlying

mechanisms involved in tumor response to hyperthermia, especially involved in hyperthermia resistance, are still poorly understood.

Cirbp belongs to the family of cold shock proteins that are activated under cold stress[15-21]. Therapeutic hypothermia protected photoreceptors through activating Cirbp pathway[25], while Cirbp exerts neuroprotective effect during therapeutic hypothermia[111]. In addition to cold stress, heat stress also modulates Cirbp expression[26-29]. In this study, the mRNA and protein expression of Cirbp were significantly down-regulated within a short time after heating treatment, suggesting that Cirbp might act as an acute phase protein in cancer cells under heat stress. A previous study showed that heat treatment also down-regulated Cirbp expression in prostate cancer cells[29]. Moreover, heat-induced Cirbp downregulation was observed in the testes of mice and humans under heat stress condition[26-28]. These aforementioned findings suggest that Cirbp might be involved in regulating the response of tumor cells to hyperthermia. In this study, our results from in vitro and in vivo experiments demonstrated that Cirbp suppression by RNAi significantly improved the sensitivity of cancer cells and cancer stem-like cells to hyperthermia. On the contrary, exogenous expression of Cirbp almost completely compromised the anti-tumor-killing effect of hyperthermia against cancer cells and cancer stem-like cells in vitro and in vivo, suggesting that ectopic expression of Cirbp induces hyperthermia resistance. Altogether, this work is the first to uncover a previously unrecognized role of Cirbp in regulating hyperthermia resistance and hyperthermic sensitization in cancer.

Of particular interest is how ectopic expression of Cirbp causes hyperthermia resistance and Cirbp silencing sensitizes NPC cells to hyperthermia. Cirbp that is initially described as a DNA damage-induced transcript is a stress-induced protein[19]. Cirbp has been implicated in DNA damage and repair[15, 19, 98, 99], while recent study reported that PARP-1-dependent recruitment of Cirbp promotes double-strand break (DSB) repair and genome stability[15]. Upon hyperthermia-induced DNA damage, tumor cells utilize two primarily distinct kinase signaling cascades to repair DSBs, including the ATM-Chk2 and ATR-Chk1 axes[97, 100-105]. Moreover, Cirbp plays a crucial role in mediating the associations of MRN and ATM with chromatin[15]. Our results clearly demonstrated that Cirbp knockdown significantly repressed ATM-Chk2 and ATR-Chk1 pathways after hyperthermia, and consequently attenuated DNA damage repair ability of cancer cells and seriously impaired cancer cell survival, ultimately enhancing thermosensitivity in cancer cells and cancer stem-like cells, and tumor growth inhibition (Figure 9). Conversely, our data showed that during hyperthermia treatment, ectopic expression of Cirbp completely or mostly rescued hyperthermia-induced reduction in the phosphorylation levels of ATM, Chk2, p53, ATR and Chk1, which thereby reversed hyperthermia-induced reduction in DNA damage repair ability of cancer cells and increase in cell apoptosis, ultimately leading to increased thermoresistance and tumor growth, indicating that Cirbp overexpression protects cancer cells against hyperthermia-induced DNA damage and cell death (Figure 9). Together, these data suggest, for the first time, that exogenous expression of Cirbp induces hyperthermia resistance by promoting DNA damage repair in cancer cells, whereas Cirbp silencing can sensitize cancer cells and cancer stem-like cells to hyperthermic therapy via attenuating the ability of DNA damage repair.

It is well known that CSCs contribute to the resistance to conventional anticancer treatments, such as radiotherapy, chemotherapy, immunotherapy and hyperthermia therapy[7, 73-81]. The previous studies showed that moderate low temperature preserved the stemness of neural stem cells (NSCs) and prevented cell apoptosis via activation of Cirbp[112], while forced expression of Cirbp under hypoxia could restore the proliferation of NSCs[113], suggesting the importance of Cirbp in the stemness maintenance and self-renewal of stem cells. However, to date, it is still unknown how Cirbp functions in CSCs. Actually, our findings from this study, for the first time, revealed that Cirbp suppression significantly attenuated the stemness property of cancer cells, which thereby contributed to noticeably improving the sensitivity of cancer stem-like cells to hyperthermia. On the contrast, this work is the first to reveal that ectopic expression of Cirbp mostly or completely compromised hyperthermia-induced reduction in the stemness of cancer cells, which thereby contributed to the resistance of cancer stem-like cells to hyperthermia. It is clear that our above findings are in line with the functions of Cirbp on stemness in NSCs[112, 113]. Since CSCs are responsible for the resistance to anticancer therapy, such as hyperthermia therapy[7, 73-81], the functions of Cirbp in the stemness maintenance of CSCs also contributes to the hyperthermia resistance or hyperthermic radiosensitization in our study.

It is well known that a single miRNA can regulate a large number of target protein-coding genes involved in different signal transduction pathways that participate in many physiological and pathological processes, including tumor formation and progression[45, 85-89]. Therefore, miRNAs are being considered as potential therapeutic targets for various diseases, including hepatitis and cancers[45, 85-89]. Several miRNA mimics and molecules that target miRNAs (anti-miRs) have shown promise for clinical application in preclinical or clinical trials[90, 91], and miRNA-targeted therapeutics have already been tested in clinical trials, including a mimic of the tumor suppressor miR-34, which reached phase I clinical trials for cancer treatment[90] and anti-miRs targeting miR-122, which reached phase II trials for hepatitis treatment[114]. More importantly, in vitro chemical synthesis and in vivo delivery of miRNAs for cancer therapy is very handy[45, 85-89]. In addition, the previous study indicated that some miRNAs (i.e., miR-142-5p and miR-143) were identified to belong to temperature-sensitive miRNAs (termed thermomiRs)[83]. In this study, Cirbp is identified to be a direct target of thermomiR-377-3p in NPC cells, while thermomiR-377–3p improves the sensitivity of NPC cells and cancer stem-like cells to hyperthermia by directly suppressing Cirbp expression, suggesting that thermomiR-377–3p is a promising therapeutic targets of hyperthermia for NPC.

The use of hyperthermia as a treatment for cancer is not new and dates back to the work of Coley[115, 116], which has a wide variety of biological effects. In recent years, a large number of in vitro and in vivo experiments and clinical data demonstrate that as an adjunctive therapy, hyperthermia combined with radiotherapy and-/or chemotherapy improves clinical outcome in cancer therapy[1-4]. More specifically, hyperthermia has been confirmed to improve response to chemoradiation therapy in patients with soft tissue sarcoma[117], liver cancer[118] and comprehensively raise therapeutic effect to radiation in several clinical trials in patients who have head and neck[119, 120], melanoma[121], breast[122-124], advanced cervical[125-127] and brain cancer[128-130]. Currently, the standard therapy for patients with NPC is radiotherapy combined with chemotherapy[30-32]. In contrast to other solid

cancers[1-10], the hyperthermia is relatively less investigated in NPC. In the field of NPC, a small amount of clinical trials preliminarily demonstrated that hyperthermia combined with radiation therapy can improve progression-free survival and local progression-free survival of NPC patients, although no increase in overall survival was observed[33-36]. In this study, our findings firstly revealed that hyperthermia dramatically attenuated the stemness property of NPC cells, while combination treatment of hyperthermia and Ori significantly increased the anti-tumor killing effect on NPC cells and CSC-like population within NPC cells. Moreover, our results also indicated that hyperthermia substantially improved the sensitivity of radiation-resistant NPC cells and CSC-like cells to radiotherapy. Collectively, this work is first to uncover that hyperthermia alone or combined with radiotherapy or chemotherapy can effectively eliminate CSC-like population within NPC cells.

Natural product Ori is the major active ingredient of the traditional Chinese medicinal herb Rabdosia rubescens, and has anti-tumor activity [58-72] and anti-inflammatory[131]. Ori and its analogue alone or combined with chemotherapy and radiotherapy was reported to effectively kill tumor cells of leukemia, ovarian cancer, lung cancer, esophageal squamous cell carcinoma, osteosarcoma, breast cancer, colorectal cancer and prostate cancer [58-72]. As CSCs have been identified as the main center of cancer therapeutic resistance[132-134], eradicating CSCs is considered as an effective and powerful strategy to improve current anti-cancer therapeutics[132-134]. However, it remains unknown whether Ori and its analogue alone or combined with hyperthermia can effectively kill CSCs. Our work is the first to reveal that Ori treatment alone or combined with hyperthermia effectively eliminates CSC-like population within cancer cells, suggesting that Ori is active against cancer stem-like cells, but the targets of Ori remain to be fully investigated.

Conclusions

In summary, this work is the first to identify a previously unrecognized mechanism of hyperthermia resistance that Cirbp causes hyperthermia resistance by enhancing DNA damage repair in cancer. ThermomiR-377–3p and its target gene Cirbp are important regulators of thermosensitivity and may represent important targets of hyperthermia for further development.

Abbreviations

Cirbp: cold-inducible RNA binding protein; NPC: nasopharyngeal carcinoma; HT: hyperthermia; RT: radiotherapy; Ori: oridonin; RBM3: RNA binding motif protein 3; IF: Immunofluorescent; qRT-PCR: quantitative real-time PCR; CCK-8: cell counting kit-8; HNC: head and neck cancer; CSPs: cold shock proteins; PDT: photodynamic therapy; NIR: near-infrared; NSCs: neural stem cells; HCC: hepatocellular carcinoma; CSC: cancer stem cell.

Declarations

Acknowledgements

We thank Prof. Andrea Ventura (Memorial Sloan Kettering Cancer Center) and Prof. Jeng-Shin Lee (Harvard Gene Therapy Initiative, Harvard Medical School) for generously providing plasmids. We also thank every member of Dr. Dong Xiao's lab for their helpful discussion and suggestions.

Authors' contributions

DX and YS conducted and supervised the experiments; DX, YS, TYL, BXZ, WHH, JY, LXL, JSJ, WRL and SJX designed the experiments; TYL, JY, JSJ, SJX, JWX, ZHZ, HFS, CZ, ZZY, WQY, LBC, YLY, SWX, SJL, YL, QWL, YLL, FW, XXR, XJL and LXL jointly performed the experiments; WRL, LXL, SJX, JWX, WHH and BXZ contributed critical reagents/materials/analysis tools; DX, YS, TYL, ZHZ, SJX, JSJ, LXL, WHH, BXZ and WRL analyzed, interpreted the data and drafted the manuscript. All authors read and approved the final manuscript.

Funding

This work was supported by the National Natural Science Foundation of China (Grant No. 81872209, 82173299, 81672689, 81372896 and 81172587, to D. Xiao; Grant No. 81600086 and 81770100, to Y. Sun; Grant No. 81600488 and 81870602, to X.-L. Lin; Grant No. 81702778, to J.S. Jia; Grant No. 82060500, 81760491 and 81560441, to S.J. Xiao; Grant No. 81872202, to W.R. Luo), the Natural Science Foundation of Guangdong Province of China (Grant No. 2014A030313294 to D. Xiao; Grant No. 2018A030313778, to W.R. Luo), the President Foundation of Nanfang Hospital(Grant No.2020C002 to T.Y. Lin), Southern Medical University, the Science and Technology Planning Project of Guangdong Province of China (Grant No. 2017A010105017, 2013B060300013 and 2009B060300008, to D. Xiao; Grant No. 2017A030303018, to J.S. Jia; Grant No. 2015A030302024, to X.-L. Lin), the China Postdoctoral Science Foundation (Grant No. 2015M572338, 2016T90792, 2017M622740 and 2018T110884, to X.-L. Lin), Natural Science Foundation of Shenzhen (Grant No. JCYJ20190809154603583, to W.R. Luo), the Medical Scientific Research Foundation of Guangdong Province of China (Grant No. A2017420, to J.S. Jia), the Basic Research Foundation of Yunnan Province Local Universities (Grant No. 202001BA070001-063 to JWX) and the Science and Technology Planning Project of Kunming City of China (Grant No. 2019-1-S-25318000001329 to JWX).

Availability of data and materials

All data generated or analyzed during the current study are included in this published article (and its supplementary information files).

Consent for publication

The authors confirm that they have obtained written consent from each patient to publish the manuscript.

Competing interests

The authors declare that they have no competing interests.

References

[1] K. Ahmed, Y. Tabuchi, T. Kondo, Hyperthermia: an effective strategy to induce apoptosis in cancer cells, Apoptosis : an international journal on programmed cell death, 20 (2015) 1411-1419.

[2] M.W. Dewhirst, C.T. Lee, K.A. Ashcraft, The future of biology in driving the field of hyperthermia, International journal of hyperthermia : the official journal of European Society for Hyperthermic Oncology, North American Hyperthermia Group, 32 (2016) 4-13.

[3] J.K. Kang, J.C. Kim, Y. Shin, S.M. Han, W.R. Won, J. Her, J.Y. Park, K.T. Oh, Principles and applications of nanomaterial-based hyperthermia in cancer therapy, Archives of pharmacal research, 43 (2020) 46-57.

[4] G. Lassche, J. Crezee, C.M.L. Van Herpen, Whole-body hyperthermia in combination with systemic therapy in advanced solid malignancies, Critical reviews in oncology/hematology, 139 (2019) 67-74.

[5] J. Beik, Z. Abed, F.S. Ghoreishi, S. Hosseini-Nami, S. Mehrzadi, A. Shakeri-Zadeh, S.K. Kamrava, Nanotechnology in hyperthermia cancer therapy: From fundamental principles to advanced applications, Journal of controlled release : official journal of the Controlled Release Society, 235 (2016) 205-221.

[6] N.R. Datta, S. Krishnan, D.E. Speiser, E. Neufeld, N. Kuster, S. Bodis, H. Hofmann, Magnetic nanoparticle-induced hyperthermia with appropriate payloads: Paul Ehrlich's "magic (nano)bullet" for cancer theranostics?, Cancer treatment reviews, 50 (2016) 217-227.

[7] H. Ghaffari, J. Beik, A. Talebi, S.R. Mahdavi, H. Abdollahi, New physical approaches to treat cancer stem cells: a review, Clinical & translational oncology : official publication of the Federation of Spanish Oncology Societies and of the National Cancer Institute of Mexico, 20 (2018) 1502-1521.

[8] I. Pereira Gomes, J. Aparecida Duarte, A.L. Chaves Maia, D. Rubello, D.M. Townsend, A.L. Branco de Barros, E.A. Leite, Thermosensitive Nanosystems Associated with Hyperthermia for Cancer Treatment, Pharmaceuticals, 12 (2019).

[9] A. Sohail, Z. Ahmad, O.A. Beg, S. Arshad, L. Sherin, A review on hyperthermia via nanoparticle-mediated therapy, Bulletin du cancer, 104 (2017) 452-461.

[10] X. Wang, L. Cheng, Multifunctional two-dimensional nanocomposites for photothermal-based combined cancer therapy, Nanoscale, 11 (2019) 15685-15708.

[11] M. Agarwal, S. Pandita, C.R. Hunt, A. Gupta, X. Yue, S. Khan, R.K. Pandita, D. Pratt, J.W. Shay, J.S. Taylor, T.K. Pandita, Inhibition of telomerase activity enhances hyperthermia-mediated radiosensitization, Cancer research, 68 (2008) 3370-3378.

[12] J. Man, J.D. Shoemake, T. Ma, A.E. Rizzo, A.R. Godley, Q. Wu, A.M. Mohammadi, S. Bao, J.N. Rich, J.S. Yu, Hyperthermia Sensitizes Glioma Stem-like Cells to Radiation by Inhibiting AKT Signaling, Cancer research, 75 (2015) 1760-1769.

[13] H. Hatakeyama, S.Y. Wu, Y.A. Lyons, S. Pradeep, W. Wang, Q. Huang, K.A. Court, T. Liu, S. Nie, C. Rodriguez-Aguayo, F. Shen, Y. Huang, T. Hisamatsu, T. Mitamura, N. Jennings, J. Shim, P.L. Dorniak, L.S. Mangala, M. Petrillo, V.A. Petyuk, A.A. Schepmoes, A.K. Shukla, M. Torres-Lugo, J.S. Lee, K.D. Rodland, A. Fagotti, G. Lopez-Berestein, C. Li, A.K. Sood, Role of CTGF in Sensitivity to Hyperthermia in Ovarian and Uterine Cancers, Cell reports, 17 (2016) 1621-1631.

[14] L. Schaaf, M. Schwab, C. Ulmer, S. Heine, T.E. Murdter, J.O. Schmid, G. Sauer, W.E. Aulitzky, H. van der Kuip, Hyperthermia Synergizes with Chemotherapy by Inhibiting PARP1-Dependent DNA Replication Arrest, Cancer research, 76 (2016) 2868-2875.

[15] J.K. Chen, W.L. Lin, Z. Chen, H.W. Liu, PARP-1-dependent recruitment of cold-inducible RNA-binding protein promotes double-strand break repair and genome stability, Proceedings of the National Academy of Sciences of the United States of America, 115 (2018) E1759-E1768.

[16] Y. Liao, L. Tong, L. Tang, S. Wu, The role of cold-inducible RNA binding protein in cell stress response, International journal of cancer, 141 (2017) 2164-2173.

[17] T.Y. Lin, Y. Chen, J.S. Jia, C. Zhou, M. Lian, Y.T. Wen, X.Y. Li, H.W. Chen, X.L. Lin, X.L. Zhang, S.J. Xiao, Y. Sun, D. Xiao, Loss of Cirbp expression is correlated with the malignant progression and poor prognosis in nasopharyngeal carcinoma, Cancer management and research, 11 (2019) 6959-6969.

[18] M. Lu, Q. Ge, G. Wang, Y. Luo, X. Wang, W. Jiang, X. Liu, C.L. Wu, Y. Xiao, X. Wang, CIRBP is a novel oncogene in human bladder cancer inducing expression of HIF-1alpha, Cell death & disease, 9 (2018) 1046.

[19] D.A. Lujan, J.L. Ochoa, R.S. Hartley, Cold-inducible RNA binding protein in cancer and inflammation, Wiley interdisciplinary reviews. RNA, 9 (2018).

[20] P. Zhong, H. Huang, Recent progress in the research of cold-inducible RNA-binding protein, Future science OA, 3 (2017) FSO246.

[21] X. Zhu, C. Buhrer, S. Wellmann, Cold-inducible proteins CIRP and RBM3, a unique couple with activities far beyond the cold, Cellular and molecular life sciences : CMLS, 73 (2016) 3839-3859.

[22] M. Aziz, M. Brenner, P. Wang, Extracellular CIRP (eCIRP) and inflammation, Journal of leukocyte biology, 106 (2019) 133-146.

[23] M.M. Hoekstra, Y. Emmenegger, J. Hubbard, P. Franken, Cold-inducible RNA-binding protein (CIRBP) adjusts clock-gene expression and REM-sleep recovery following sleep deprivation, eLife, 8 (2019).

[24] Y. Liu, J. Xing, Y. Li, Q. Luo, Z. Su, X. Zhang, H. Zhang, Chronic hypoxia-induced Cirbp hypermethylation attenuates hypothermic cardioprotection via down-regulation of ubiquinone biosynthesis, Science translational medicine, 11 (2019).

[25] Y.J. Sun, S. Ma, B. Fan, Y. Wang, S.R. Wang, G.Y. Li, Therapeutic hypothermia protects photoreceptors through activating Cirbp pathway, Neurochemistry international, 126 (2019) 86-95.

[26] M. Rao, D. Ke, G. Cheng, S. Hu, Y. Wu, Y. Wang, F. Zhou, H. Liu, C. Zhu, W. Xia, The regulation of CIRBP by transforming growth factor beta during heat shock-induced testicular injury, Andrology, 7 (2019) 244-250.

[27] G. Cheng, D. Ke, M. Rao, S. Hu, Y. Wang, F. Zhou, H. Liu, C. Zhu, W. Xia, Effects of cold-inducible RNA-binding protein on the proliferation and apoptosis of spermatogenic cells in vitro following heat stress, Reproduction, fertility, and development, 31 (2019) 953-961.

[28] H. Nishiyama, S. Danno, Y. Kaneko, K. Itoh, H. Yokoi, M. Fukumoto, H. Okuno, J.L. Millan, T. Matsuda, O. Yoshida, J. Fujita, Decreased expression of cold-inducible RNA-binding protein (CIRP) in male germ cells at elevated temperature, The American journal of pathology, 152 (1998) 289-296.

[29] Y. Zeng, P. Kulkarni, T. Inoue, R.H. Getzenberg, Down-regulating cold shock protein genes impairs cancer cell survival and enhances chemosensitivity, Journal of cellular biochemistry, 107 (2009) 179-188.

[30] Y.P. Chen, A.T.C. Chan, Q.T. Le, P. Blanchard, Y. Sun, J. Ma, Nasopharyngeal carcinoma, Lancet, 394 (2019) 64-80.

[31] M.L.K. Chua, J.T.S. Wee, E.P. Hui, A.T.C. Chan, Nasopharyngeal carcinoma, Lancet, 387 (2016) 1012-1024.

[32] X.R. Tang, Y.Q. Li, S.B. Liang, W. Jiang, F. Liu, W.X. Ge, L.L. Tang, Y.P. Mao, Q.M. He, X.J. Yang, Y. Zhang, X. Wen, J. Zhang, Y.Q. Wang, P.P. Zhang, Y. Sun, J.P. Yun, J. Zeng, L. Li, L.Z. Liu, N. Liu, J. Ma, Development and validation of a gene expression-based signature to predict distant metastasis in locoregionally advanced nasopharyngeal carcinoma: a retrospective, multicentre, cohort study, The Lancet. Oncology, 19 (2018) 382-393.

[33] Y. Hua, S. Ma, Z. Fu, Q. Hu, L. Wang, Y. Piao, Intracavity hyperthermia in nasopharyngeal cancer: a phase III clinical study, International journal of hyperthermia : the official journal of European Society for Hyperthermic Oncology, North American Hyperthermia Group, 27 (2011) 180-186.

[34] M. Kang, W.Q. Liu, Y.T. Qin, Z.X. Wei, R.S. Wang, Long-term efficacy of microwave hyperthermia combined with chemoradiotherapy in treatment of nasopharyngeal carcinoma with cervical lymph node metastases, Asian Pacific journal of cancer prevention : APJCP, 14 (2013) 7395-7400.

[35] M.M. Paulides, G.C. Van Rhoon, Towards developing effective hyperthermia treatment for tumours in the nasopharyngeal region, International journal of hyperthermia : the official journal of European Society for Hyperthermic Oncology, North American Hyperthermia Group, 27 (2011) 523-525; author reply 526.

[36] Q.L. Wen, L.J. He, P.R. Ren, C.Q. Chen, J.B. Wu, Comparing radiotherapy with or without intracavitary hyperthermia in the treatment of primary nasopharyngeal carcinoma: a retrospective analysis, Tumori,

100 (2014) 49-54.

[37] Y. Chen, X. Deng, W. Chen, P. Shi, M. Lian, H. Wang, K. Wang, D. Qian, D. Xiao, H. Long, Silencing of microRNA-708 promotes cell growth and epithelial-to-mesenchymal transition by activating the SPHK2/AKT/beta-catenin pathway in glioma, Cell death & disease, 10 (2019) 448.

[38] X. Lin, J. Jia, T. Du, W. Li, X. Wang, J. Wei, X. Lin, H. Zeng, L. Yao, X. Chen, J. Zhuang, J. Weng, Y. Liu, J. Lin, Q. Wu, W. Wang, K. Yao, K. Xu, D. Xiao, Overexpression of miR-155 in the liver of transgenic mice alters the expression profiling of hepatic genes associated with lipid metabolism, PLoS ONE, 10 (2015) e0118417.

[39] X. Li, Z. Zhao, X. Zhang, S. Yang, X. Lin, X. Yang, X. Lin, J. Shi, S. Wang, W. Zhao, J. Li, F. Gao, M. Liu, N. Ma, W. Luo, K. Yao, Y. Sun, S. Xiao, D. Xiao, J. Jia, Klf4 reduces stemness phenotype, triggers mesenchymal-epithelial transition (MET)-like molecular changes, and prevents tumor progression in nasopharygeal carcinoma, Oncotarget, 8 (2017) 93924-93941.

[40] X. Lin, Y. Qin, J. Jia, T. Lin, X. Lin, L. Chen, H. Zeng, Y. Han, L. Wu, S. Huang, M. Wang, S. Huang, R. Xie, L. Liang, Y. Liu, R. Liu, T. Zhang, J. Li, S. Wang, P. Sun, W. Huang, K. Yao, K. Xu, T. Du, D. Xiao, MiR-155 Enhances Insulin Sensitivity by Coordinated Regulation of Multiple Genes in Mice, PLoS genetics, 12 (2016) e1006308.

[41] J.W. Shi, T.T. Zhang, W. Liu, J. Yang, X.L. Lin, J.S. Jia, H.F. Shen, S.C. Wang, J. Li, W.T. Zhao, W.W. Gu, Y. Sun, D. Xiao, Direct conversion of pig fibroblasts to chondrocyte-like cells by c-Myc, Cell death discovery, 5 (2019) 55.

[42] Y. Sun, D. Xiao, H.A. Li, J.F. Jiang, Q. Li, R.S. Zhang, X.G. Chen, Phenotypic changes of human cells in human-rat liver during partial hepatectomy-induced regeneration, World journal of gastroenterology, 15 (2009) 3611-3620.

[43] S.C. Wang, X.L. Lin, H.Y. Wang, Y.J. Qin, L. Chen, J. Li, J.S. Jia, H.F. Shen, S. Yang, R.Y. Xie, F. Wei, F. Gao, X.X. Rong, J. Yang, W.T. Zhao, T.T. Zhang, J.W. Shi, K.T. Yao, W.R. Luo, Y. Sun, D. Xiao, Hes1 triggers epithelial-mesenchymal transition (EMT)-like cellular marker alterations and promotes invasion and metastasis of nasopharyngeal carcinoma by activating the PTEN/AKT pathway, Oncotarget, 6 (2015) 36713-36730.

[44] R. Xie, X. Lin, T. Du, K. Xu, H. Shen, F. Wei, W. Hao, T. Lin, X. Lin, Y. Qin, H. Wang, L. Chen, S. Yang, J. Yang, X. Rong, K. Yao, D. Xiao, J. Jia, Y. Sun, Targeted Disruption of miR-17-92 Impairs Mouse Spermatogenesis by Activating mTOR Signaling Pathway, Medicine, 95 (2016) e2713.

[45] W.T. Zhao, X.L. Lin, Y. Liu, L.X. Han, J. Li, T.Y. Lin, J.W. Shi, S.C. Wang, M. Lian, H.W. Chen, Y. Sun, K. Xu, J.S. Jia, R.C. Luo, D. Xiao, miR-26a promotes hepatocellular carcinoma invasion and metastasis by inhibiting PTEN and inhibits cell growth by repressing EZH2, Laboratory investigation; a journal of technical methods and pathology, 99 (2019) 1484-1500.

[46] J. Li, S. Yang, W. Yan, J. Yang, Y.J. Qin, X.L. Lin, R.Y. Xie, S.C. Wang, W. Jin, F. Gao, J.W. Shi, W.T. Zhao, J.S. Jia, H.F. Shen, J.R. Ke, B. Liu, Y.Q. Zhao, W.H. Huang, K.T. Yao, D.J. Li, D. Xiao, MicroRNA-19 triggers epithelial-mesenchymal transition of lung cancer cells accompanied by growth inhibition, Laboratory investigation; a journal of technical methods and pathology, 95 (2015) 1056-1070.

[47] X. Lin, L. Chen, H. Li, Y. Liu, Y. Guan, X. Li, Z. Jia, X. Lin, J. Jia, Y. Sun, D. Xiao, miR-155 accelerates proliferation of mouse hepatocytes during liver regeneration by directly targeting SOCS1, American journal of physiology. Gastrointestinal and liver physiology, 315 (2018) G443-g453.

[48] S.C. Wang, X.L. Lin, J. Li, T.T. Zhang, H.Y. Wang, J.W. Shi, S. Yang, W.T. Zhao, R.Y. Xie, F. Wei, Y.J. Qin, L. Chen, J. Yang, K.T. Yao, D. Xiao, MicroRNA-122 triggers mesenchymal-epithelial transition and suppresses hepatocellular carcinoma cell motility and invasion by targeting RhoA, PLoS ONE, 9 (2014) e101330.

[49] X.X. Rong, F. Wei, X.L. Lin, Y.J. Qin, L. Chen, H.Y. Wang, H.F. Shen, L.T. Jia, R.Y. Xie, T.Y. Lin, W.C. Hao, J. Yang, S. Yang, Y.S. Cheng, W.H. Huang, A.M. Li, Y. Sun, R.C. Luo, D. Xiao, Recognition and killing of cancer stem-like cell population in hepatocellular carcinoma cells by cytokine-induced killer cells via NKG2d-ligands recognition, Oncoimmunology, 5 (2016) e1086060.

[50] F. Wei, X.X. Rong, R.Y. Xie, L.T. Jia, H.Y. Wang, Y.J. Qin, L. Chen, H.F. Shen, X.L. Lin, J. Yang, S. Yang, W.C. Hao, Y. Chen, S.J. Xiao, H.R. Zhou, T.Y. Lin, Y.S. Chen, Y. Sun, K.T. Yao, D. Xiao, Cytokine-induced killer cells efficiently kill stem-like cancer cells of nasopharyngeal carcinoma via the NKG2D-ligands recognition, Oncotarget, 6 (2015) 35023-35039.

[51] J.W. Shi, W. Liu, T.T. Zhang, S.C. Wang, X.L. Lin, J. Li, J.S. Jia, H.F. Sheng, Z.F. Yao, W.T. Zhao, Z.L. Zhao, R.Y. Xie, S. Yang, F. Gao, Q.R. Fan, M.Y. Zhang, M. Yue, J. Yuan, W.W. Gu, K.T. Yao, D. Xiao, The enforced expression of c-Myc in pig fibroblasts triggers mesenchymal-epithelial transition (MET) via F-actin reorganization and RhoA/Rock pathway inactivation, Cell cycle (Georgetown, Tex.), 12 (2013) 1119-1127.

[52] P. Chomczynski, N. Sacchi, Single-step method of RNA isolation by acid guanidinium thiocyanate-phenol-chloroform extraction, Analytical biochemistry, 162 (1987) 156-159.

[53] M. Hou, C. Yan, Z. Chen, Q. Zhao, M. Yuan, Y. Xu, B. Zhao, Multifunctional NIR-responsive poly(vinylpyrrolidone)-Cu-Sb-S nanotheranostic agent for photoacoustic imaging and photothermal/photodynamic therapy, Acta biomaterialia, 74 (2018) 334-343.

[54] G. Dontu, W.M. Abdallah, J.M. Foley, K.W. Jackson, M.F. Clarke, M.J. Kawamura, M.S. Wicha, In vitro propagation and transcriptional profiling of human mammary stem/progenitor cells, Genes & development, 17 (2003) 1253-1270.

[55] Q.L. Kong, L.J. Hu, J.Y. Cao, Y.J. Huang, L.H. Xu, Y. Liang, D. Xiong, S. Guan, B.H. Guo, H.Q. Mai, Q.Y. Chen, X. Zhang, M.Z. Li, J.Y. Shao, C.N. Qian, Y.F. Xia, L.B. Song, Y.X. Zeng, M.S. Zeng, Epstein-Barr virus-

encoded LMP2A induces an epithelial-mesenchymal transition and increases the number of side population stem-like cancer cells in nasopharyngeal carcinoma, PLoS pathogens, 6 (2010) e1000940.

[56] J. Wang, L.P. Guo, L.Z. Chen, Y.X. Zeng, S.H. Lu, Identification of cancer stem cell-like side population cells in human nasopharyngeal carcinoma cell line, Cancer research, 67 (2007) 3716-3724.

[57] P.K. Lo, D. Kanojia, X. Liu, U.P. Singh, F.G. Berger, Q. Wang, H. Chen, CD49f and CD61 identify Her2/neu-induced mammary tumor-initiating cells that are potentially derived from luminal progenitors and maintained by the integrin-TGFbeta signaling, Oncogene, 31 (2012) 2614-2626.

[58] H.L. Huang, H.Y. Weng, L.Q. Wang, C.H. Yu, Q.J. Huang, P.P. Zhao, J.Z. Wen, H. Zhou, L.H. Qu, Triggering Fbw7-mediated proteasomal degradation of c-Myc by oridonin induces cell growth inhibition and apoptosis, Molecular cancer therapeutics, 11 (2012) 1155-1165.

[59] S. Li, D. Shi, L. Zhang, F. Yang, G. Cheng, Oridonin enhances the radiosensitivity of lung cancer cells by upregulating Bax and downregulating Bcl-2, Experimental and therapeutic medicine, 16 (2018) 4859-4864.

[60] Y. Lu, Y. Sun, J. Zhu, L. Yu, X. Jiang, J. Zhang, X. Dong, B. Ma, Q. Zhang, Oridonin exerts anticancer effect on osteosarcoma by activating PPAR-gamma and inhibiting Nrf2 pathway, Cell death & disease, 9 (2018) 15.

[61] H. Luo, C.T. Vong, H. Chen, Y. Gao, P. Lyu, L. Qiu, M. Zhao, Q. Liu, Z. Cheng, J. Zou, P. Yao, C. Gao, J. Wei, C.O.L. Ung, S. Wang, Z. Zhong, Y. Wang, Naturally occurring anti-cancer compounds: shining from Chinese herbal medicine, Chinese medicine, 14 (2019) 48.

[62] M. Ming, F.Y. Sun, W.T. Zhang, J.K. Liu, Therapeutic effect of oridonin on mice with prostate cancer, Asian Pacific journal of tropical medicine, 9 (2016) 184-187.

[63] B.A. Owona, H.J. Schluesener, Molecular Insight in the Multifunctional Effects of Oridonin, Drugs in R&D, 15 (2015) 233-244.

[64] X. Shen, L. Zhao, P. Chen, Y. Gong, D. Liu, X. Zhang, L. Dai, Q. Sun, J. Lou, Z. Jin, B. Zhang, D. Niu, C. Chen, X. Qi, D. Jia, A thiazole-derived oridonin analogue exhibits antitumor activity by directly and allosterically inhibiting STAT3, The Journal of biological chemistry, 294 (2019) 17471-17486.

[65] M. Song, X. Liu, K. Liu, R. Zhao, H. Huang, Y. Shi, M. Zhang, S. Zhou, H. Xie, H. Chen, Y. Li, Y. Zheng, Q. Wu, F. Liu, E. Li, A.M. Bode, Z. Dong, M.H. Lee, Targeting AKT with Oridonin Inhibits Growth of Esophageal Squamous Cell Carcinoma In Vitro and Patient-Derived Xenografts In Vivo, Molecular cancer therapeutics, 17 (2018) 1540-1553.

[66] M. Vasaturo, R. Cotugno, L. Fiengo, C. Vinegoni, F. Dal Piaz, N. De Tommasi, The anti-tumor diterpene oridonin is a direct inhibitor of Nucleolin in cancer cells, Scientific reports, 8 (2018) 16735.

[67] H. Weng, H. Huang, B. Dong, P. Zhao, H. Zhou, L. Qu, Inhibition of miR-17 and miR-20a by oridonin triggers apoptosis and reverses chemoresistance by derepressing BIM-S, Cancer research, 74 (2014) 4409-4419.

[68] S. Xu, H. Yao, M. Hu, D. Li, Z. Zhu, W. Xie, H. Yao, L. Wu, Z.S. Chen, J. Xu, 6,7-Seco-ent-Kauranoids Derived from Oridonin as Potential Anticancer Agents, J Nat Prod, 80 (2017) 2391-2398.

[69] Y. Xu, J. Liu, Y. Wu, Q. Guo, H. Sun, G. Chen, Natural products against hematological malignancies and identification of their targets, Science China. Life sciences, 58 (2015) 1191-1201.

[70] Z. Yao, F. Xie, M. Li, Z. Liang, W. Xu, J. Yang, C. Liu, H. Li, H. Zhou, L.H. Qu, Oridonin induces autophagy via inhibition of glucose metabolism in p53-mutated colorectal cancer cells, Cell death & disease, 8 (2017) e2633.

[71] Y. Zhao, H. Xia, Oridonin elevates sensitivity of ovarian carcinoma cells to cisplatin via suppressing cisplatin-mediated autophagy, Life sciences, 233 (2019) 116709.

[72] T. Zhen, C.F. Wu, P. Liu, H.Y. Wu, G.B. Zhou, Y. Lu, J.X. Liu, Y. Liang, K.K. Li, Y.Y. Wang, Y.Y. Xie, M.M. He, H.M. Cao, W.N. Zhang, L.M. Chen, K. Petrie, S.J. Chen, Z. Chen, Targeting of AML1-ETO in t(8;21) leukemia by oridonin generates a tumor suppressor-like protein, Science translational medicine, 4 (2012) 127ra138.

[73] E. Bessede, C. Staedel, L.A. Acuna Amador, P.H. Nguyen, L. Chambonnier, M. Hatakeyama, G. Belleannee, F. Megraud, C. Varon, Helicobacter pylori generates cells with cancer stem cell properties via epithelial-mesenchymal transition-like changes, Oncogene, 33 (2014) 4123-4131.

[74] S.Y. Lee, E.K. Jeong, M.K. Ju, H.M. Jeon, M.Y. Kim, C.H. Kim, H.G. Park, S.I. Han, H.S. Kang, Induction of metastasis, cancer stem cell phenotype, and oncogenic metabolism in cancer cells by ionizing radiation, Molecular cancer, 16 (2017) 10.

[75] S.A. Mani, W. Guo, M.J. Liao, E.N. Eaton, A. Ayyanan, A.Y. Zhou, M. Brooks, F. Reinhard, C.C. Zhang, M. Shipitsin, L.L. Campbell, K. Polyak, C. Brisken, J. Yang, R.A. Weinberg, The epithelial-mesenchymal transition generates cells with properties of stem cells, Cell, 133 (2008) 704-715.

[76] G.S. Markopoulos, E. Roupakia, K.B. Marcu, E. Kolettas, Epigenetic Regulation of Inflammatory Cytokine-Induced Epithelial-To-Mesenchymal Cell Transition and Cancer Stem Cell Generation, Cells, 8 (2019).

[77] M. Najafi, B. Farhood, K. Mortezaee, Cancer stem cells (CSCs) in cancer progression and therapy, Journal of cellular physiology, 234 (2019) 8381-8395.

[78] X. Jiao, X. Qian, L. Wu, B. Li, Y. Wang, X. Kong, L. Xiong, microRNA: The Impact on Cancer Stemness and Therapeutic Resistance, Cells, 9 (2019).

[79] M.R. Atashzar, R. Baharlou, J. Karami, H. Abdollahi, R. Rezaei, F. Pourramezan, S.H. Zoljalali Moghaddam, Cancer stem cells: A review from origin to therapeutic implications, Journal of cellular physiology, 235 (2020) 790-803.

[80] R.L. Bighetti-Trevisan, L.O. Sousa, R.M. Castilho, L.O. Almeida, Cancer Stem Cells: Powerful Targets to Improve Current Anticancer Therapeutics, Stem cells international, 2019 (2019) 9618065.

[81] F.Y. Du, Q.F. Zhou, W.J. Sun, G.L. Chen, Targeting cancer stem cells in drug discovery: Current state and future perspectives, World journal of stem cells, 11 (2019) 398-420.

[82] M.E. Lleonart, A new generation of proto-oncogenes: cold-inducible RNA binding proteins, Biochimica et biophysica acta, 1805 (2010) 43-52.

[83] J.J. Wong, A.Y. Au, D. Gao, N. Pinello, C.T. Kwok, A. Thoeng, K.A. Lau, J.E. Gordon, U. Schmitz, Y. Feng, T.V. Nguyen, R. Middleton, C.G. Bailey, J. Holst, J.E. Rasko, W. Ritchie, RBM3 regulates temperature sensitive miR-142-5p and miR-143 (thermomiRs), which target immune genes and control fever, Nucleic acids research, 44 (2016) 2888-2897.

[84] G. Tong, N.N.A. von Garlen, S.J. Wowro, P.D. Lam, J. Krech, F. Berger, K.R.L. Schmitt, Post-TTM Rebound Pyrexia after Ischemia-Reperfusion Injury Results in Sterile Inflammation and Apoptosis in Cardiomyocytes, Mediators of inflammation, 2019 (2019) 6431957.

[85] S. Biswas, MicroRNAs as Therapeutic Agents: The Future of the Battle Against Cancer, Current topics in medicinal chemistry, 18 (2018) 2544-2554.

[86] C.M. Croce, Causes and consequences of microRNA dysregulation in cancer, Nature reviews. Genetics, 10 (2009) 704-714.

[87] R. Garzon, G.A. Calin, C.M. Croce, MicroRNAs in Cancer, Annual review of medicine, 60 (2009) 167-179.

[88] A. Nadeem, M.R. Ashraf, M. Javed, T. Hussain, M.S. Tariq, M.E. Babar, Review - MicroRNAs: A new paradigm towards mechanistic insight of diseases, Pakistan journal of pharmaceutical sciences, 31 (2018) 2017-2026.

[89] K. Saliminejad, H.R. Khorram Khorshid, S. Soleymani Fard, S.H. Ghaffari, An overview of microRNAs: Biology, functions, therapeutics, and analysis methods, Journal of cellular physiology, 234 (2019) 5451-5465.

[90] H. Ling, M. Fabbri, G.A. Calin, MicroRNAs and other non-coding RNAs as targets for anticancer drug development, Nature reviews. Drug discovery, 12 (2013) 847-865.

[91] R. Rupaimoole, F.J. Slack, MicroRNA therapeutics: towards a new era for the management of cancer and other diseases, Nature reviews. Drug discovery, 16 (2017) 203-222.

[92] K.D. Barnes, G. Shafirstein, J.S. Webber, N.A. Koonce, Z. Harris, R.J. Griffin, Hyperthermia-enhanced indocyanine green delivery for laser-induced thermal ablation of carcinomas, International journal of hyperthermia : the official journal of European Society for Hyperthermic Oncology, North American Hyperthermia Group, 29 (2013) 474-479.

[93] G. Sheng, Y. Chen, L. Han, Y. Huang, X. Liu, L. Li, Z. Mao, Encapsulation of indocyanine green into cell membrane capsules for photothermal cancer therapy, Acta biomaterialia, 43 (2016) 251-261.

[94] C. Shirata, J. Kaneko, Y. Inagaki, T. Kokudo, M. Sato, S. Kiritani, N. Akamatsu, J. Arita, Y. Sakamoto, K. Hasegawa, N. Kokudo, Near-infrared photothermal/photodynamic therapy with indocyanine green induces apoptosis of hepatocellular carcinoma cells through oxidative stress, Scientific reports, 7 (2017) 13958.

[95] G. Wan, B. Chen, L. Li, D. Wang, S. Shi, T. Zhang, Y. Wang, L. Zhang, Y. Wang, Nanoscaled red blood cells facilitate breast cancer treatment by combining photothermal/photodynamic therapy and chemotherapy, Biomaterials, 155 (2018) 25-40.

[96] N. Zhang, M. Li, X. Sun, H. Jia, W. Liu, NIR-responsive cancer cytomembrane-cloaked carrier-free nanosystems for highly efficient and self-targeted tumor drug delivery, Biomaterials, 159 (2018) 25-36.

[97] Y.Y. Zhao, Q. Wu, Z.B. Wu, J.J. Zhang, L.C. Zhu, Y. Yang, S.L. Ma, S.R. Zhang, Microwave hyperthermia promotes caspase3-dependent apoptosis and induces G2/M checkpoint arrest via the ATM pathway in nonsmall cell lung cancer cells, Int J Oncol, 53 (2018) 539-550.

[98] H.N. Lee, S.M. Ahn, H.H. Jang, Cold-inducible RNA-binding protein, CIRP, inhibits DNA damage-induced apoptosis by regulating p53, Biochemical and biophysical research communications, 464 (2015) 916-921.

[99] Z. Li, E.K. Fan, J. Liu, M.J. Scott, Y. Li, S. Li, W. Xie, T.R. Billiar, M.A. Wilson, Y. Jiang, P. Wang, J. Fan, Cold-inducible RNA-binding protein through TLR4 signaling induces mitochondrial DNA fragmentation and regulates macrophage cell death after trauma, Cell death & disease, 8 (2017) e2775.

[100] L. Gong, Q. Zhang, X. Pan, S. Chen, L. Yang, B. Liu, W. Yang, L. Yu, Z.X. Xiao, X.H. Feng, H. Wang, Z.M. Yuan, J. Peng, W.Q. Tan, J. Chen, p53 Protects Cells from Death at the Heatstroke Threshold Temperature, Cell reports, 29 (2019) 3693-3707 e3695.

[101] J. Guan, E. Stavridi, D.B. Leeper, G. Iliakis, Effects of hyperthermia on p53 protein expression and activity, Journal of cellular physiology, 190 (2002) 365-374.

[102] C.R. Hunt, R.K. Pandita, A. Laszlo, R. Higashikubo, M. Agarwal, T. Kitamura, A. Gupta, N. Rief, N. Horikoshi, R. Baskaran, J.H. Lee, M. Lobrich, T.T. Paull, J.L. Roti Roti, T.K. Pandita, Hyperthermia activates a subset of ataxia-telangiectasia mutated effectors independent of DNA strand breaks and heat shock protein 70 status, Cancer research, 67 (2007) 3010-3017.

[103] J. Smith, L.M. Tho, N. Xu, D.A. Gillespie, The ATM-Chk2 and ATR-Chk1 pathways in DNA damage signaling and cancer, Advances in cancer research, 108 (2010) 73-112.

[104] M. Tomita, Involvement of DNA-PK and ATM in radiation- and heat-induced DNA damage recognition and apoptotic cell death, Journal of radiation research, 51 (2010) 493-501.

[105] M. Tuul, H. Kitao, M. Iimori, K. Matsuoka, S. Kiyonari, H. Saeki, E. Oki, M. Morita, Y. Maehara, Rad9, Rad17, TopBP1 and claspin play essential roles in heat-induced activation of ATR kinase and heat tolerance, PloS one, 8 (2013) e55361.

[106] X. Liu, Y. Zhang, Y. Wang, W. Zhu, G. Li, X. Ma, Y. Zhang, S. Chen, S. Tiwari, K. Shi, S. Zhang, H.M. Fan, Y.X. Zhao, X.J. Liang, Comprehensive understanding of magnetic hyperthermia for improving antitumor therapeutic efficacy, Theranostics, 10 (2020) 3793-3815.

[107] K.A. Court, H. Hatakeyama, S.Y. Wu, M.S. Lingegowda, C. Rodriguez-Aguayo, G. Lopez-Berestein, L. Ju-Seog, C. Rinaldi, E.J. Juan, A.K. Sood, M. Torres-Lugo, HSP70 Inhibition Synergistically Enhances the Effects of Magnetic Fluid Hyperthermia in Ovarian Cancer, Molecular cancer therapeutics, 16 (2017) 966-976.

[108] J. Shao, B. Han, P. Cao, B. Zhang, M. Liu, D. Li, N. Zhou, Q. Hao, X. Duan, Y. Chang, A. Nakai, Y. Fan, K. Tan, HSF1 phosphorylation by cyclosporin A confers hyperthermia sensitivity through suppression of HSP expression, Biochimica et biophysica acta. Gene regulatory mechanisms, 1862 (2019) 846-857.

[109] L.E.M. Vriend, N. van den Tempel, A.L. Oei, M. L'Acosta, F.J. Pieterson, N.A.P. Franken, R. Kanaar, P.M. Krawczyk, Boosting the effects of hyperthermia-based anticancer treatments by HSP90 inhibition, Oncotarget, 8 (2017) 97490-97503.

[110] C. Mu, X. Wu, X. Zhou, J. Wolfram, J. Shen, D. Zhang, J. Mai, X. Xia, A.M. Holder, M. Ferrari, X. Liu, H. Shen, Chemotherapy Sensitizes Therapy-Resistant Cells to Mild Hyperthermia by Suppressing Heat Shock Protein 27 Expression in Triple-Negative Breast Cancer, Clinical cancer research : an official journal of the American Association for Cancer Research, 24 (2018) 4900-4912.

[111] L. Wu, H.L. Sun, Y. Gao, K.L. Hui, M.M. Xu, H. Zhong, M.L. Duan, Therapeutic Hypothermia Enhances Cold-Inducible RNA-Binding Protein Expression and Inhibits Mitochondrial Apoptosis in a Rat Model of Cardiac Arrest, Molecular neurobiology, 54 (2017) 2697-2705.

[112] K. Saito, N. Fukuda, T. Matsumoto, Y. Iribe, A. Tsunemi, T. Kazama, C. Yoshida-Noro, N. Hayashi, Moderate low temperature preserves the stemness of neural stem cells and suppresses apoptosis of the cells via activation of the cold-inducible RNA binding protein, Brain research, 1358 (2010) 20-29.

[113] Q. Zhang, Y.Z. Wang, W. Zhang, X. Chen, J. Wang, J. Chen, W. Luo, Involvement of Cold Inducible RNA-Binding Protein in Severe Hypoxia-Induced Growth Arrest of Neural Stem Cells In Vitro, Molecular neurobiology, 54 (2017) 2143-2153.

[114] H.L. Janssen, H.W. Reesink, E.J. Lawitz, S. Zeuzem, M. Rodriguez-Torres, K. Patel, A.J. van der Meer, A.K. Patick, A. Chen, Y. Zhou, R. Persson, B.D. King, S. Kauppinen, A.A. Levin, M.R. Hodges, Treatment of HCV infection by targeting microRNA, The New England journal of medicine, 368 (2013) 1685-1694.

[115] W.B. Coley, The Treatment of Inoperable Sarcoma by Bacterial Toxins (the Mixed Toxins of the Streptococcus erysipelas and the Bacillus prodigiosus), Proceedings of the Royal Society of Medicine, 3 (1910) 1-48.

[116] L.R. Zacharski, V.P. Sukhatme, Coley's toxin revisited: immunotherapy or plasminogen activator therapy of cancer?, Journal of thrombosis and haemostasis : JTH, 3 (2005) 424-427.

[117] T. Lim, I. Lee, J. Kim, W.K. Kang, Synergistic Effect of Simvastatin Plus Radiation in Gastric Cancer and Colorectal Cancer: Implications of BIRC5 and Connective Tissue Growth Factor, International journal of radiation oncology, biology, physics, 93 (2015) 316-325.

[118] F.K. Storm, L.R. Kaiser, J.E. Goodnight, W.H. Harrison, R.S. Elliott, A.S. Gomes, D.L. Morton, Thermochemotherapy for melanoma metastases in liver, Cancer, 49 (1982) 1243-1248.

[119] N.R. Datta, A.K. Bose, H.K. Kapoor, S. Gupta, Head and neck cancers: results of thermoradiotherapy versus radiotherapy, International journal of hyperthermia : the official journal of European Society for Hyperthermic Oncology, North American Hyperthermia Group, 6 (1990) 479-486.

[120] R. Valdagni, M. Amichetti, Report of long-term follow-up in a randomized trial comparing radiation therapy and radiation therapy plus hyperthermia to metastatic lymph nodes in stage IV head and neck patients, International journal of radiation oncology, biology, physics, 28 (1994) 163-169.

[121] J. Overgaard, D. Gonzalez Gonzalez, M.C. Hulshof, G. Arcangeli, O. Dahl, O. Mella, S.M. Bentzen, Randomised trial of hyperthermia as adjuvant to radiotherapy for recurrent or metastatic malignant melanoma. European Society for Hyperthermic Oncology, Lancet, 345 (1995) 540-543.

[122] C.C. Vernon, J.W. Hand, S.B. Field, D. Machin, J.B. Whaley, J. van der Zee, W.L. van Putten, G.C. van Rhoon, J.D. van Dijk, D. González González, F.F. Liu, P. Goodman, M. Sherar, Radiotherapy with or without hyperthermia in the treatment of superficial localized breast cancer: results from five randomized controlled trials. International Collaborative Hyperthermia Group, International journal of radiation oncology, biology, physics, 35 (1996) 731-744.

[123] E.L. Jones, J.R. Oleson, L.R. Prosnitz, T.V. Samulski, Z. Vujaskovic, D. Yu, L.L. Sanders, M.W. Dewhirst, Randomized trial of hyperthermia and radiation for superficial tumors, Journal of clinical oncology : official journal of the American Society of Clinical Oncology, 23 (2005) 3079-3085.

[124] M. Linthorst, A.N. van Geel, M. Baaijens, A. Ameziane, W. Ghidey, G.C. van Rhoon, J. van der Zee, Re-irradiation and hyperthermia after surgery for recurrent breast cancer, Radiotherapy and oncology : journal of the European Society for Therapeutic Radiology and Oncology, 109 (2013) 188-193.

[125] J. Van der Zee, G.C. Van Rhoon, M.P. Broekmeyer-Reurink, A.E. Kuijs, A.P. Van Den Berg, D. Treurniet-Donker, W.L. Van Putten, H.S. Reinhold, Clinical experience with local hyperthermia in Rotterdam, Advances in experimental medicine and biology, 267 (1990) 383-386.

[126] Y. Harima, K. Nagata, K. Harima, V.V. Ostapenko, Y. Tanaka, S. Sawada, A randomized clinical trial of radiation therapy versus thermoradiotherapy in stage IIIB cervical carcinoma, International journal of hyperthermia : the official journal of European Society for Hyperthermic Oncology, North American Hyperthermia Group, 17 (2001) 97-105.

[127] A. Zolciak-Siwinska, N. Piotrkowicz, J. Jonska-Gmyrek, M. Nicke-Psikuta, W. Michalski, M. Kawczyńska, M. Bijok, K. Bujko, HDR brachytherapy combined with interstitial hyperthermia in locally advanced cervical cancer patients initially treated with concomitant radiochemotherapy–a phase III study, Radiotherapy and oncology : journal of the European Society for Therapeutic Radiology and Oncology, 109 (2013) 194-199.

[128] P.K. Sneed, P.R. Stauffer, M.W. McDermott, C.J. Diederich, K.R. Lamborn, M.D. Prados, S. Chang, K.A. Weaver, L. Spry, M.K. Malec, S.A. Lamb, B. Voss, R.L. Davis, W.M. Wara, D.A. Larson, T.L. Phillips, P.H. Gutin, Survival benefit of hyperthermia in a prospective randomized trial of brachytherapy boost +/- hyperthermia for glioblastoma multiforme, International journal of radiation oncology, biology, physics, 40 (1998) 287-295.

[129] M.H. Falk, R.D. Issels, Hyperthermia in oncology, International journal of hyperthermia : the official journal of European Society for Hyperthermic Oncology, North American Hyperthermia Group, 17 (2001) 1-18.

[130] M.Y. Klimanov, L.A. Syvak, V.E. Orel, G.V. Lavryk, T.Y. Tarasenko, V.B. Orel, A.Y. Rykhalskyi, V.V. Stegnii, A.O. Nesterenko, Efficacy of Combined Regional Inductive Moderate Hyperthermia and Chemotherapy in Patients With Multiple Liver Metastases From Breast Cancer, Technology in cancer research & treatment, 17 (2018) 1533033818806003.

[131] H. He, H. Jiang, Y. Chen, J. Ye, A. Wang, C. Wang, Q. Liu, G. Liang, X. Deng, W. Jiang, R. Zhou, Oridonin is a covalent NLRP3 inhibitor with strong anti-inflammasome activity, Nature communications, 9 (2018) 2550.

[132] K. Dzobo, D.A. Senthebane, C. Ganz, N.E. Thomford, A. Wonkam, C. Dandara, Advances in Therapeutic Targeting of Cancer Stem Cells within the Tumor Microenvironment: An Updated Review, Cells, 9 (2020).

[133] T. Huang, X. Song, D. Xu, D. Tiek, A. Goenka, B. Wu, N. Sastry, B. Hu, S.Y. Cheng, Stem cell programs in cancer initiation, progression, and therapy resistance, Theranostics, 10 (2020) 8721-8743.

[134] H. Li, Z. Feng, M.L. He, Lipid metabolism alteration contributes to and maintains the properties of cancer stem cells, Theranostics, 10 (2020) 7053-7069.

Figures

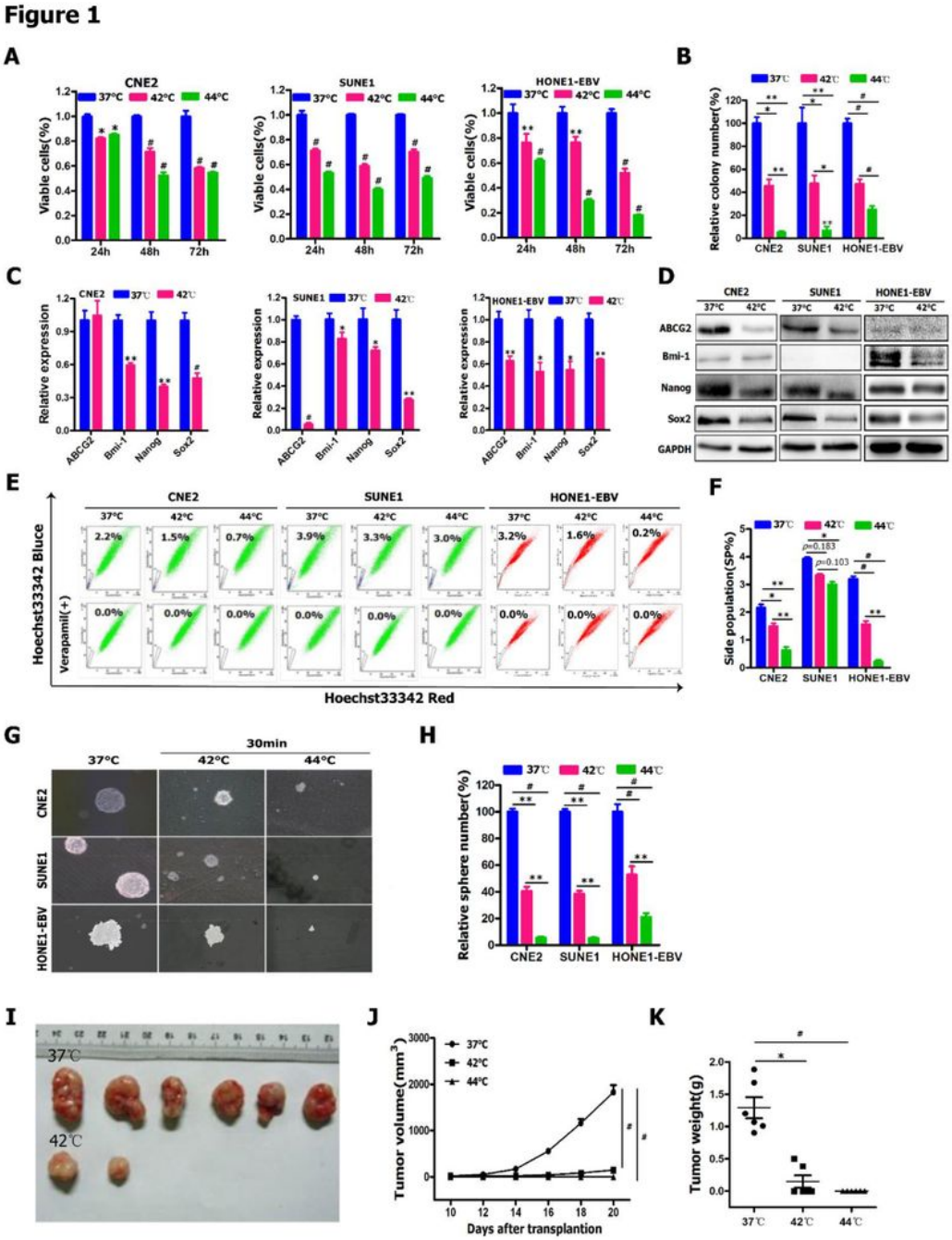

Figure 1

Hyperthermia significantly suppressed the proliferation and stemness of NPC cells. (A-B) CCK-8 assay (A) and colony formation assay (B) were performed in indicated NPC cells treated with hyperthermia at 42°C or 44°C for 30min. (C-D) qRT-PCR (C) and Western blot (D) were employed to detect stemness-related

gene expression in indicated NPC cells treated with hyperthermia at 42°C or 44°C for 30min. (E-F) Flow cytometry analysis of the percentages of side population (SP) cells in indicated NPC cells treated with hyperthermia at 42°C or 44°C for 30min. (G-H) Tumor sphere formation assay was used to detect the self-renewal ability of NPC cells treated with hyperthermia at 42°C or 44°C for 30min. Sphere size and density are shown in the left panels (G), and the number of spheres is shown in the right panels (H). (I-J) The xenograft subcutaneous tumor formation of hyperthermia-treated CNE2 cells in nude mice. CNE2 cells in vitro treated with hyperthermia at 42°C or 44°C for 30min were injected subcutaneously into nude mice (n=6). (I) Representative images of stripped xenograft tumors formed by CNE2 cells at the end of experiment. (J) The growth curve of tumor volumes. (K) Tumor weight.

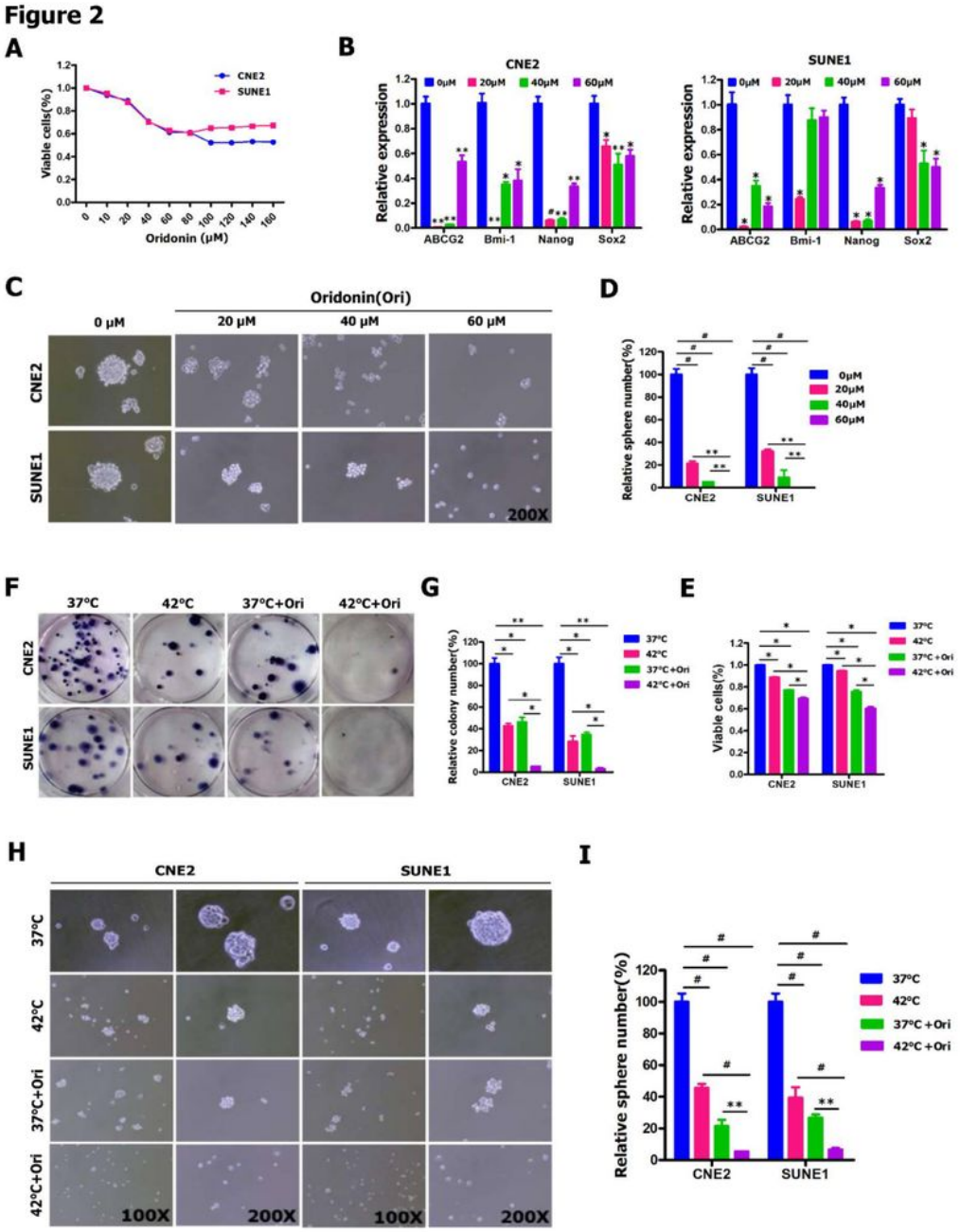

Figure 2

Combination treatment of hyperthermia and oridonin (Ori) significantly increased the killing effects on NPC cells and CSC-like population within NPC cells in vitro. (A) CCK-8 assay was performed in CNE2 and SUNE1 cells treated with oridonin at different concentrations for 24h. (B) qRT-PCR was used to detect stemness-related gene expression in CNE2 and SUNE1 cells treated with treated with different concentrations of oridonin (20, 40 and 60μM) for 24h. (C-D) Tumor sphere formation assay was

performed in CNE2 and SUNE1 cells treated with oridonin at 20, 40 and 60□M concentration for 24h. (E-I) CCK-8 assay (E), colony formation assay (F-G) and tumor sphere formation assay (H-I) were performed in CNE2 and SUNE1 cells treated with oridonin (20□M) alone or combined treated with hyperthermia (42°C for 30min).

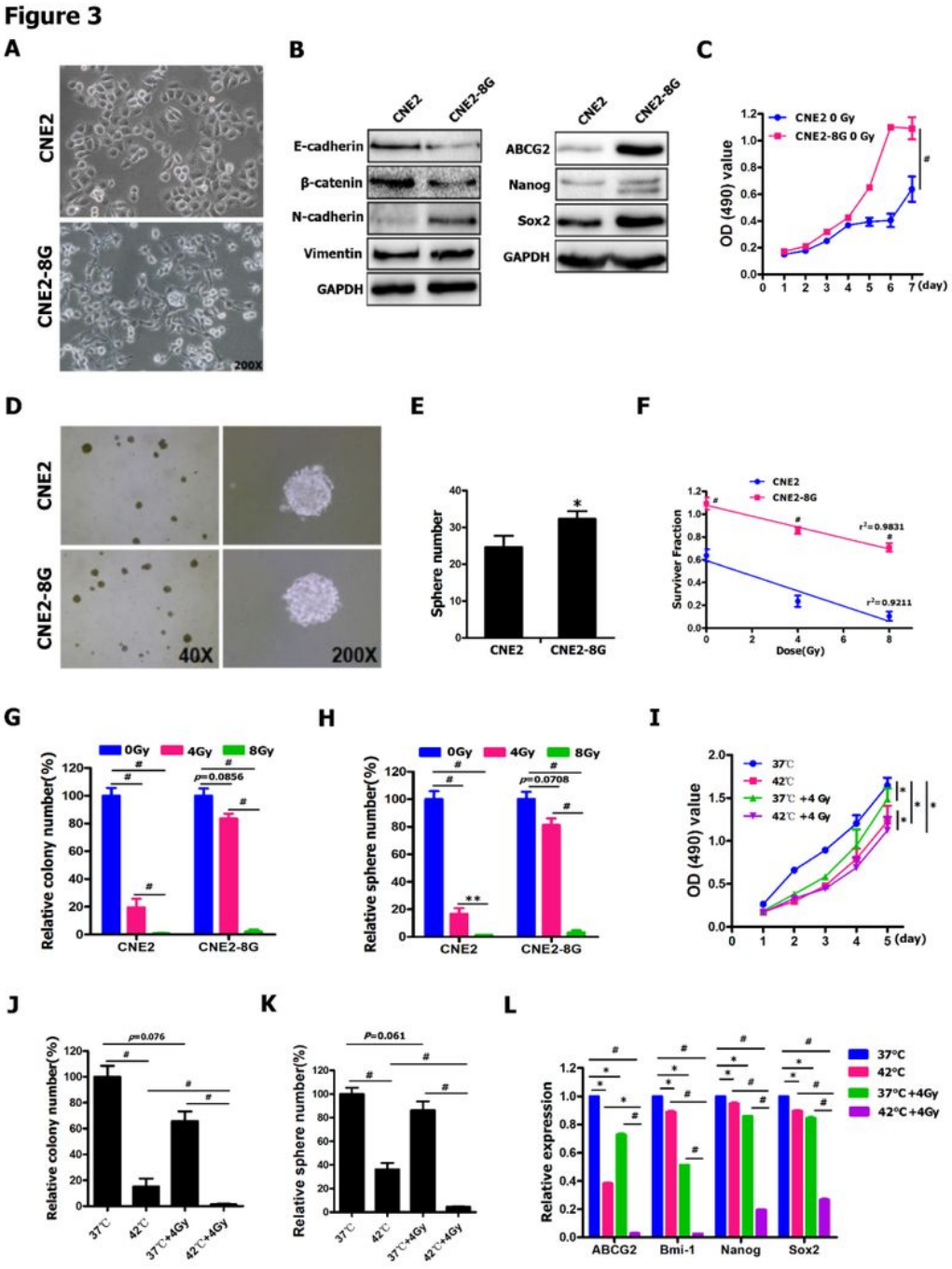

Figure 3

Hyperthermia significantly enhanced the anti-tumor-killing activity of radiotherapy against radiation-resistant NPC cells and cancer stem-like cells. (A) Representative photographs of the morphology of CNE2 cells and radiation-resistant CNE2-8G cells. (B) Western blot was employed to detect stemness- and EMT-related gene expression in CNE2 and CNE2-8G cells. (C) CCK-8 assay was performed in CNE2 and CNE2-8G cells. (D-E) Tumor sphere formation assay was performed in CNE2 and CNE2-8G cells. (F-H) CCK-8 assay (F), colony formation assay (G) and tumor sphere formation assay (H) were performed in CNE2 and CNE2-8G cells subjected to irradiation (IR) treatment at 0, 4 and 8Gy. (I-K) CCK-8 assay (I), colony formation assay (J) and tumor sphere formation assay (K) were performed in CNE2-8G cells treated by hyperthermia (42°C for 30min) and IR (4Gy) alone or combined. (L) qRT-PCR assay for detecting stemness-related gene expression in CNE2-8G cells treated by hyperthermia (42°C for 30min) and IR (4Gy) alone or combined.

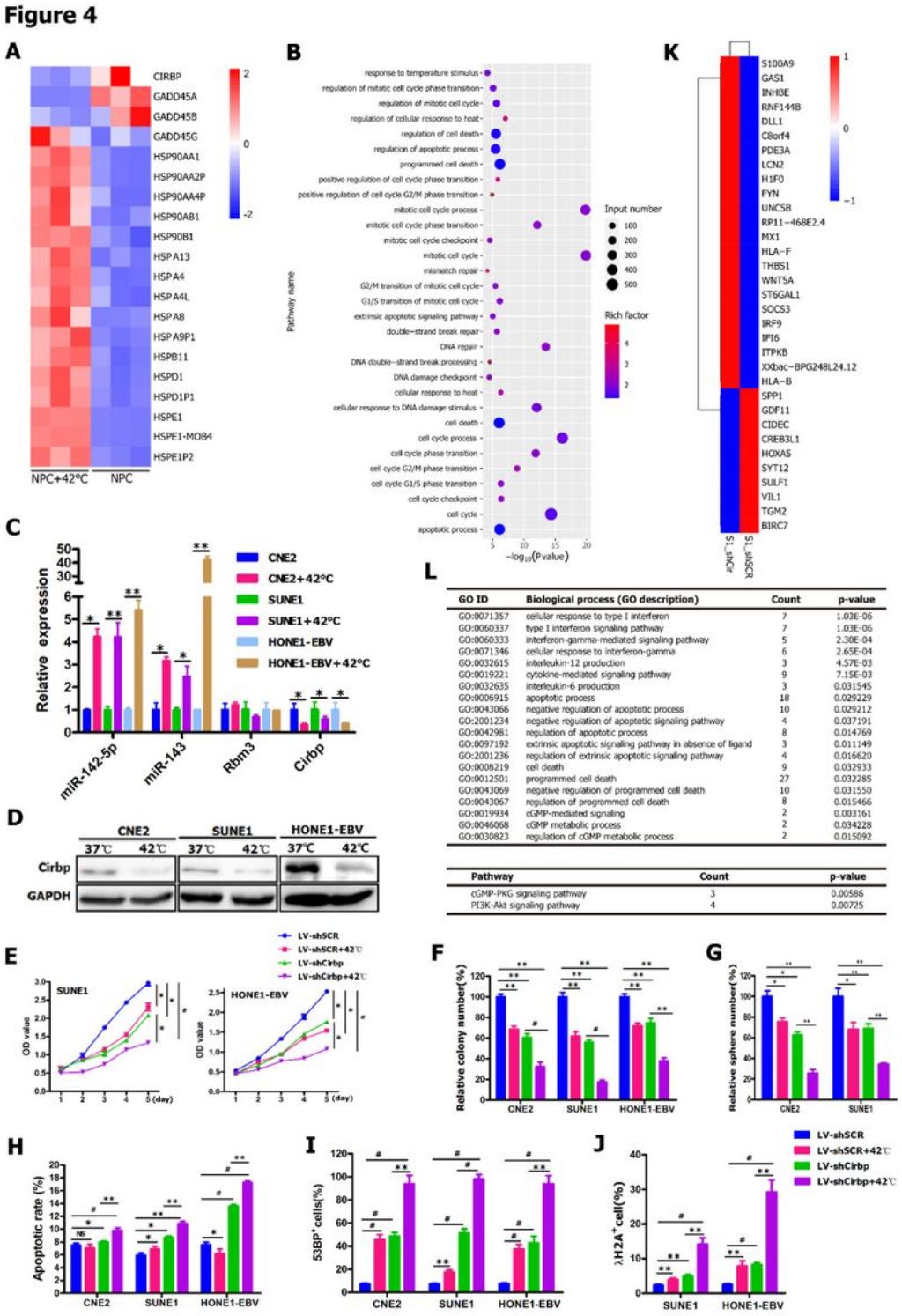

GO ID	Biological process (GO description)	Count	p-value
GO:0071357	cellular response to type I interferon	7	1.03E-06
GO:0060337	type I interferon signaling pathway	7	1.03E-06
GO:0060333	interferon-gamma-mediated signaling pathway	5	2.30E-04
GO:0071346	cellular response to interferon-gamma	6	2.65E-04
GO:0032615	interleukin-12 production	3	4.57E-03
GO:0019221	cytokine-mediated signaling pathway	9	7.15E-03
GO:0032635	interleukin-6 production	3	0.031545
GO:0006915	apoptotic process	18	0.029229
GO:0043066	negative regulation of apoptotic process	10	0.029212
GO:2001234	negative regulation of apoptotic signaling pathway	4	0.037191
GO:0042981	regulation of apoptotic process	8	0.014769
GO:0097192	extrinsic apoptotic signaling pathway in absence of ligand	3	0.011149
GO:2001236	regulation of extrinsic apoptotic signaling pathway	4	0.016620
GO:0008219	cell death	9	0.032933
GO:0012501	programmed cell death	27	0.032285
GO:0043069	negative regulation of programmed cell death	10	0.031550
GO:0043067	regulation of programmed cell death	8	0.015466
GO:0019934	cGMP-mediated signaling	2	0.003161
GO:0046068	cGMP metabolic process	2	0.034228
GO:0030823	regulation of cGMP metabolic process	2	0.015092

Pathway	Count	p-value
cGMP-PKG signaling pathway	3	0.00586
PI3K-Akt signaling pathway	4	0.00725

Figure 4

RNAi-mediated silencing of endogenous Cirbp remarkably enhanced the tumor-killing effect of hyperthermia on NPC cells and cancer stem-like cells in vitro. (A) Class comparison and hierarchical clustering of differentially expressed hyperthermia-related genes between NPC cells treated without and with hyperthermia at 42°C for 30min. A cluster heat map for 20 upregulated (red) and downregulated (blue) genes (see Table S3 and Table S4) is shown. Other details as in Fig. S6. (B) Gene ontology analysis

of up- and down-regulated genes (see Table S3) enriched in hyperthermia-associated biological processes, such as cellular response to heat, DNA damage and repair, cell cycle and cell death between NPC cells treated without and with hyperthermia at 42°C for 30min. (C) qRT-PCR assay for detecting the expression of Cirbp, Rbm3, miR-143 and miR-142-5p in the indicated NPC cells treated without or with hyperthermia at 42°C for 30min. (D) Western blot was employed to detect Cirbp expression in CNE2, SUNE1 and HONE1-EBV cells treated without or with hyperthermia at 42°C for 30min. (E-H) CCK-8 assay (E), colony formation assay (F), tumor sphere formation assay (G) and AnnexinV/PI apoptosis assay (H) were performed in shSCR- or shCirbp-expressing NPC cells treated without or with hyperthermia at 42°C for 30min. SCR: scrambled control shRNA. (I-J) Quantification of the fraction of 53BP1+ cells (I) and γ-H2AX+ cells (J) in shCirbp-expressing NPC cells treated without or with hyperthermia at 42°C for 30min are shown. Graphs represent the fraction of 53BP1+ and γ-H2AX +cells over total cell number. (K) Heatmap showing selected 35 differentially expressed genes (see Table S6) related to cell death in shCirbp-expressing NPC cells. Right column lists the selected gene symbols. (L) Gene ontology (GO) and KEGG pathway analyses of up- and down-regulated genes (see Table S6 and Table S7) related to cell survival and death in shSCR and shCirbp-expressing NPC cells.

Figure 5

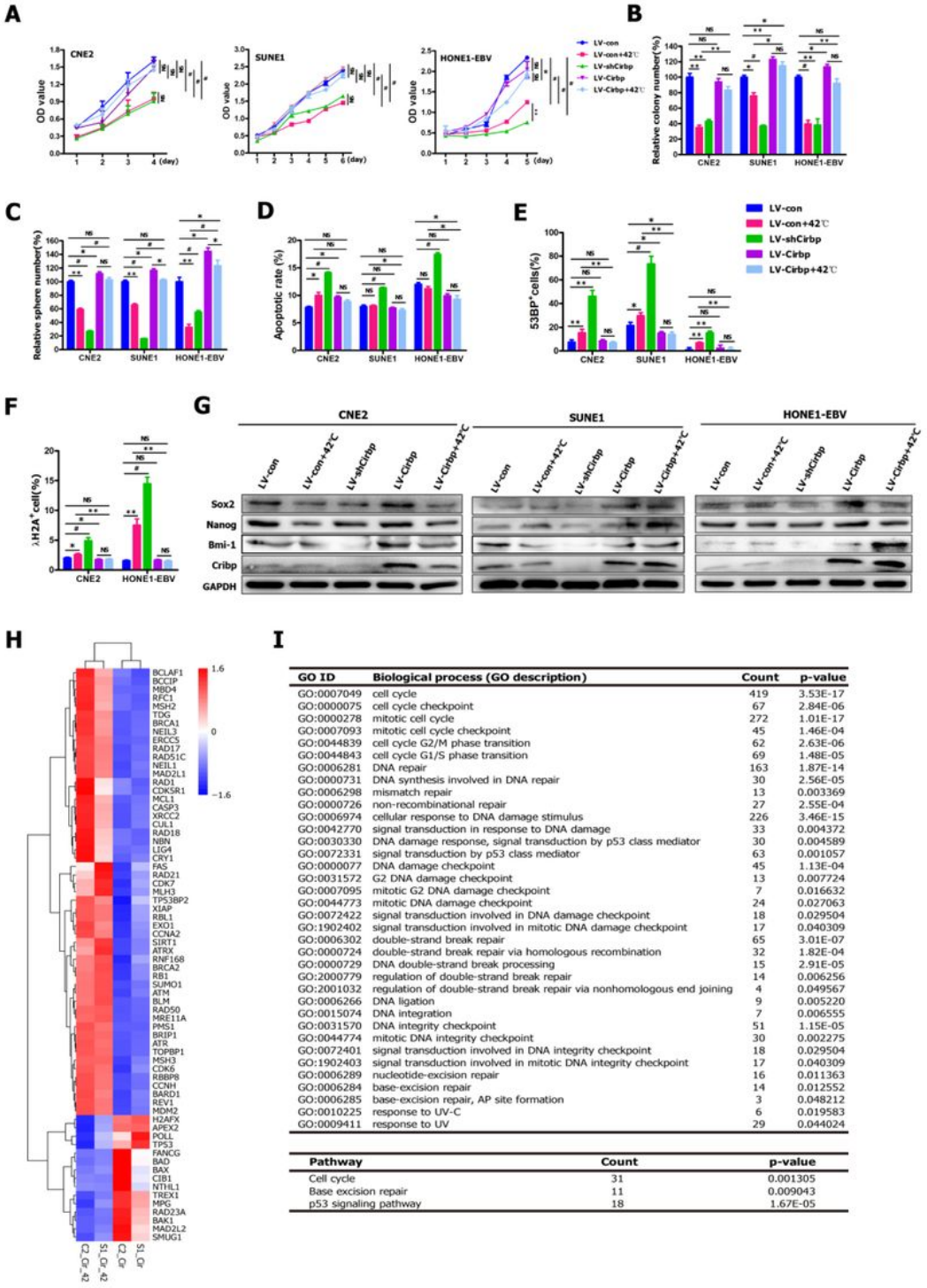

GO ID	Biological process (GO description)	Count	p-value
GO:0007049	cell cycle	419	3.53E-17
GO:0000075	cell cycle checkpoint	67	2.84E-06
GO:0000278	mitotic cell cycle	272	1.01E-17
GO:0007093	mitotic cell cycle checkpoint	45	1.46E-04
GO:0044839	cell cycle G2/M phase transition	62	2.63E-06
GO:0044843	cell cycle G1/S phase transition	69	1.48E-05
GO:0006281	DNA repair	163	1.87E-14
GO:0000731	DNA synthesis involved in DNA repair	30	2.56E-05
GO:0006298	mismatch repair	13	0.003369
GO:0000726	non-recombinational repair	27	2.55E-04
GO:0006974	cellular response to DNA damage stimulus	226	3.46E-15
GO:0042770	signal transduction in response to DNA damage	33	0.004372
GO:0030330	DNA damage response, signal transduction by p53 class mediator	30	0.004589
GO:0072331	signal transduction by p53 class mediator	63	0.001057
GO:0000077	DNA damage checkpoint	45	1.13E-04
GO:0031572	G2 DNA damage checkpoint	13	0.007724
GO:0007095	mitotic G2 DNA damage checkpoint	7	0.016632
GO:0044773	mitotic DNA damage checkpoint	24	0.027063
GO:0072422	signal transduction involved in DNA damage checkpoint	18	0.029504
GO:1902402	signal transduction involved in mitotic DNA damage checkpoint	17	0.040309
GO:0006302	double-strand break repair	65	3.01E-07
GO:0000724	double-strand break repair via homologous recombination	32	1.82E-04
GO:0000729	DNA double-strand break processing	15	2.91E-05
GO:2000779	regulation of double-strand break repair	14	0.006256
GO:2001032	regulation of double-strand break repair via nonhomologous end joining	4	0.049567
GO:0006266	DNA ligation	9	0.005220
GO:0015074	DNA integration	7	0.006555
GO:0031570	DNA integrity checkpoint	51	1.15E-05
GO:0044774	mitotic DNA integrity checkpoint	30	0.002275
GO:0072401	signal transduction involved in DNA integrity checkpoint	18	0.029504
GO:1902403	signal transduction involved in mitotic DNA integrity checkpoint	17	0.040309
GO:0006289	nucleotide-excision repair	16	0.011363
GO:0006284	base-excision repair	14	0.012552
GO:0006285	base-excision repair, AP site formation	3	0.048212
GO:0010225	response to UV-C	6	0.019583
GO:0009411	response to UV	29	0.044024

Pathway	Count	p-value
Cell cycle	31	0.001305
Base excision repair	11	0.009043
p53 signaling pathway	18	1.67E-05

Figure 5

Exogenous expression of Cirbp counteracted the tumor-killing effect of hyperthermia on NPC cells and cancer stem-like cells in vitro. (A-D) CCK-8 assay (A), colony formation assay (B), tumor sphere formation assay (C) and AnnexinV/PI apoptosis assay (D) were performed in Cirbp-expressing NPC cells treated without or with hyperthermia at 42°C for 30min. (E-F) Quantification of the fraction of 53BP1+ cells (E) and γ-H2AX+ cells (F) in Cirbp-expressing NPC cells treated without or with hyperthermia at 42°C for

30min are shown. Graphs represent the fraction of 53BP1+ and γ-H2AX + cells over total cell number. (G) Western blot analysis of stemness-related gene expression in Cirbp-expressing and shCirbp-expressing NPC cells treated without or with hyperthermia at 42°C for 30min. (H) Heatmap showing selected 35 differentially expressed genes (see Table S10) involved in DNA damage and repair, and cell cycle in Cirbp-expressing NPC cells. Right column lists the selected gene symbols. (I) Gene ontology (GO) and KEGG pathway analyses of up- and down-regulated genes (see Table S11 and Table S12) involved in DNA damage and repair, and cell cycle in Cirbp-expressing NPC cells.

Figure 6

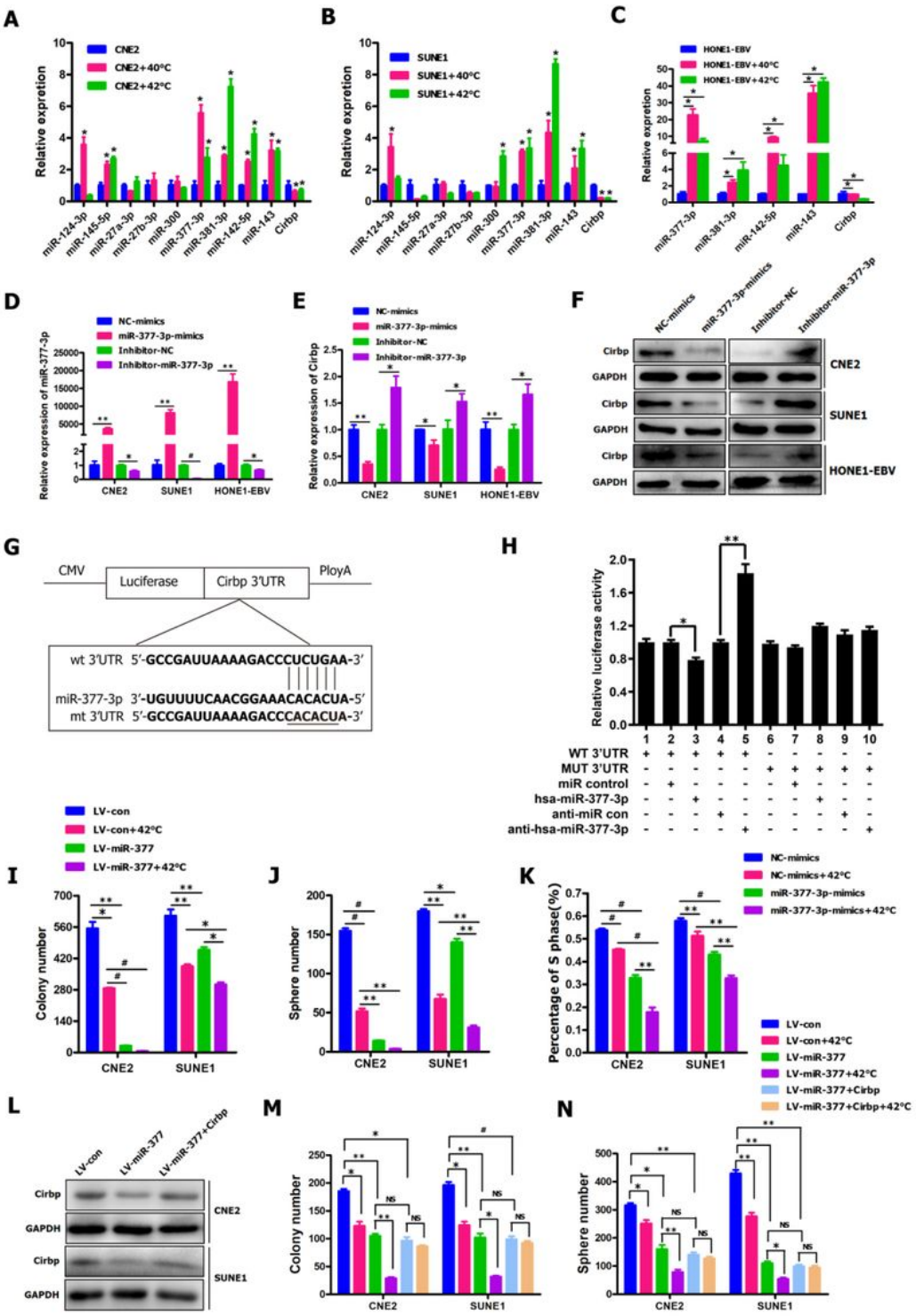

Figure 6

ThermomiR-377–3p improved the sensitivity of NPC cells and cancer stem-like cells to hyperthermia in vitro by directly suppressing Cirbp expression. (A-C) qRT-PCR assay for detecting the expression of selected miRNAs of which Cirbp might be a potential target gene in the indicated NPC cells treated without or with hyperthermia at 40°C and 42°C for 30min. ThermomiRs (i.e., miR-143 and miR-142-5p) were used as positive controls. (D-E) qRT-PCR assay for detecting the expression of miR-377-3p (D) and Cirbp (E) in NPC cells transiently transfected with miR-377-3p mimics or inhibitor. (F) Western blot was employed to detect Cirbp expression in NPC cells transiently transfected with miR-377-3p mimics or inhibitor. (G) Diagram of 3'-UTR-wt and 3'-UTR-mut of Cirbp containing reporter constructs. (H) Luciferase reporter assays in HEK293T cells co-transfected with wt or mt 3'-UTR and miRNAs as indicated. (I-J) Colony formation assay (I) and tumor sphere formation assay (J) were performed in miR-377-expressing NPC cells treated without or with hyperthermia at 42°C for 30min. (K) EdU assay was performed in NPC cells transiently transfected with miR-377-3p mimics and then treated without or with hyperthermia at 42°C for 30min. (L) Western blot was employed to detect Cirbp expression in miR-377- and Cirbp-expressing NPC cells. (M-N) Colony formation assay (M) and tumor sphere formation assay (N) were performed in miR-377- and Cirbp-expressing NPC cells treated without or with hyperthermia at 42°C for 30min.

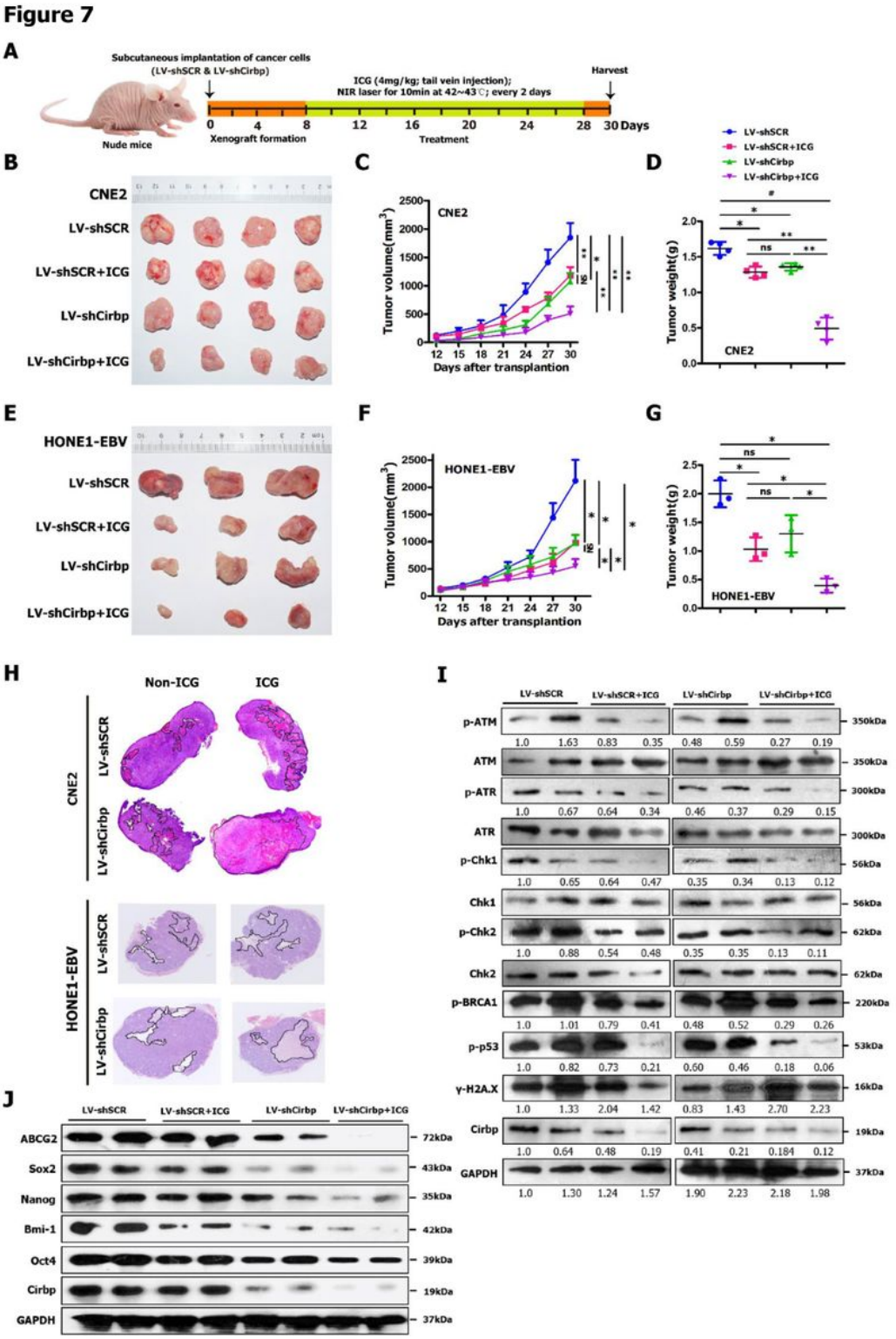

Figure 7

Cirbp silencing-induced sensitization of subcutaneous tumor xenografts to hyperthermia by local thermal ablation with ICG and an NIR laser in vivo. (A) Schematic representation of the experimental design of hyperthermia treatment in nude mice harboring subcutaneous tumor xenografts formed by CNE2 or HONE1-EBV cells. (B,E) Representative images of stripped xenograft tumors formed by CNE2 (B) and HONE1-EBV (E) cells at the end of hyperthermia therapy. (C,F) The tumor growth curve. (D,G) Tumor

weight. (H) Representative pictures of H&E staining of stripped xenograft tumors (showed in Figure 6B,E). (I) Western blot assay was used to detect Cirbp, p-ATM, p-ATR, p-Chk1, p-Chk2, p-BRCA1, p-p53 and γ-H2A.X in xenograft tumors (showed in Figure 6B) formed by CNE2 cells. (J) Western blot analysis of stemness-related gene expression in xenograft tumors (showed in Figure 6B) formed by CNE2 cells.

Figure 8

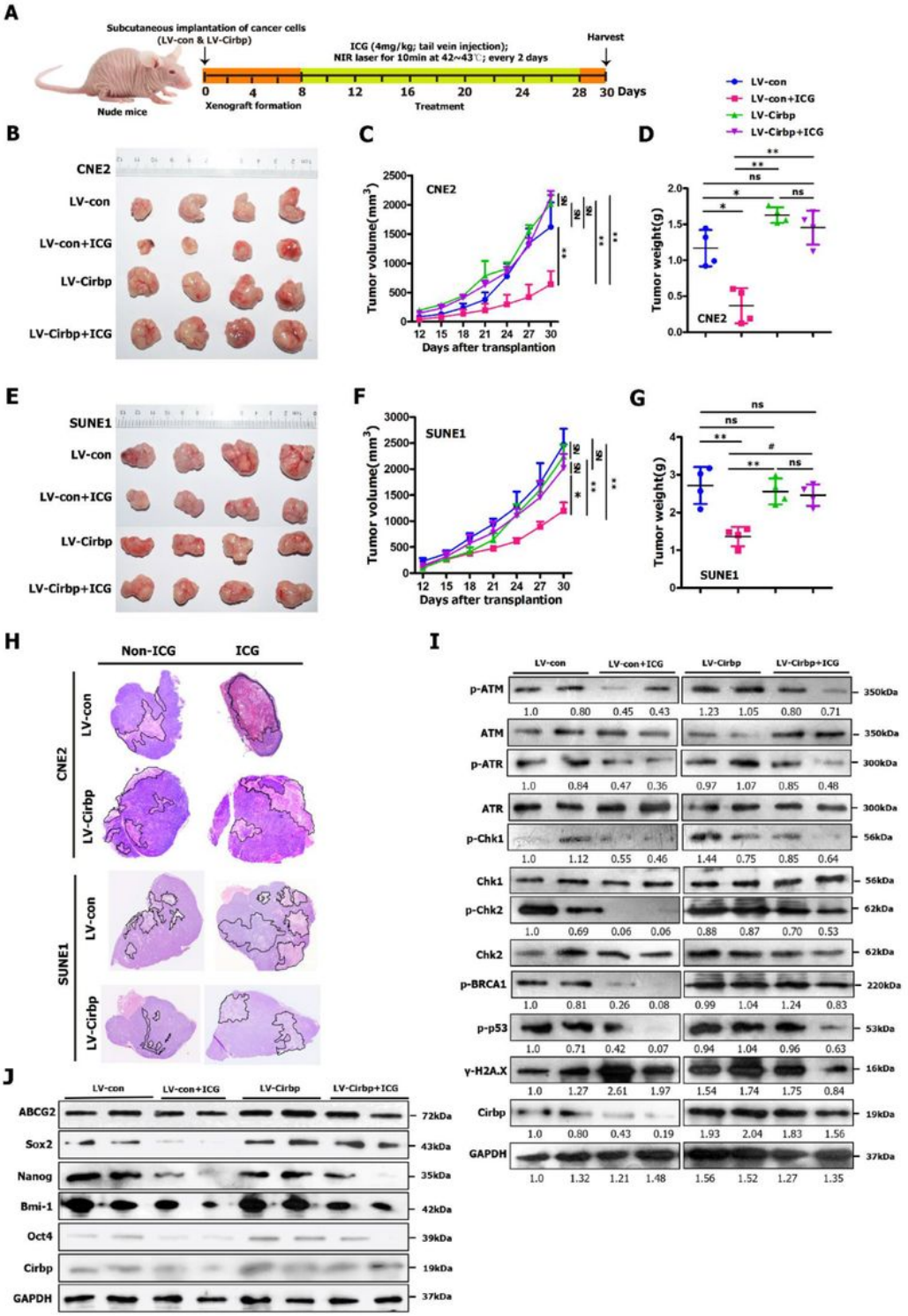

Figure 8

Ectopic expression of Cirbp counteracted the tumor-killing effect of hyperthermia on NPC cells and cancer stem-like cells in vivo. (A) Schematic representation of the experimental design of hyperthermia treatment in nude mice bearing subcutaneous tumor xenografts formed by CNE2 or SUNE1 cells. (B,E) Representative images of stripped xenograft tumors formed by CNE2 (B) and SUNE1 (E) cells at the end of hyperthermia therapy. (C,F) The tumor growth curve. (D,G) Tumor weight. (H) Representative pictures of H&E staining of stripped xenograft tumors (showed in Figure 7B,E). (I) Cirbp, p-ATM, p-ATR, p-Chk1, p-Chk2, p-BRCA1, p-p53 and γ-H2A.X in xenograft tumors (showed in Figure 7B) formed by CNE2 cells were determined by Western blot. (J) Western blot analysis of stemness-related gene expression in xenograft tumors (showed in Figure 7B) formed by CNE2 cells.

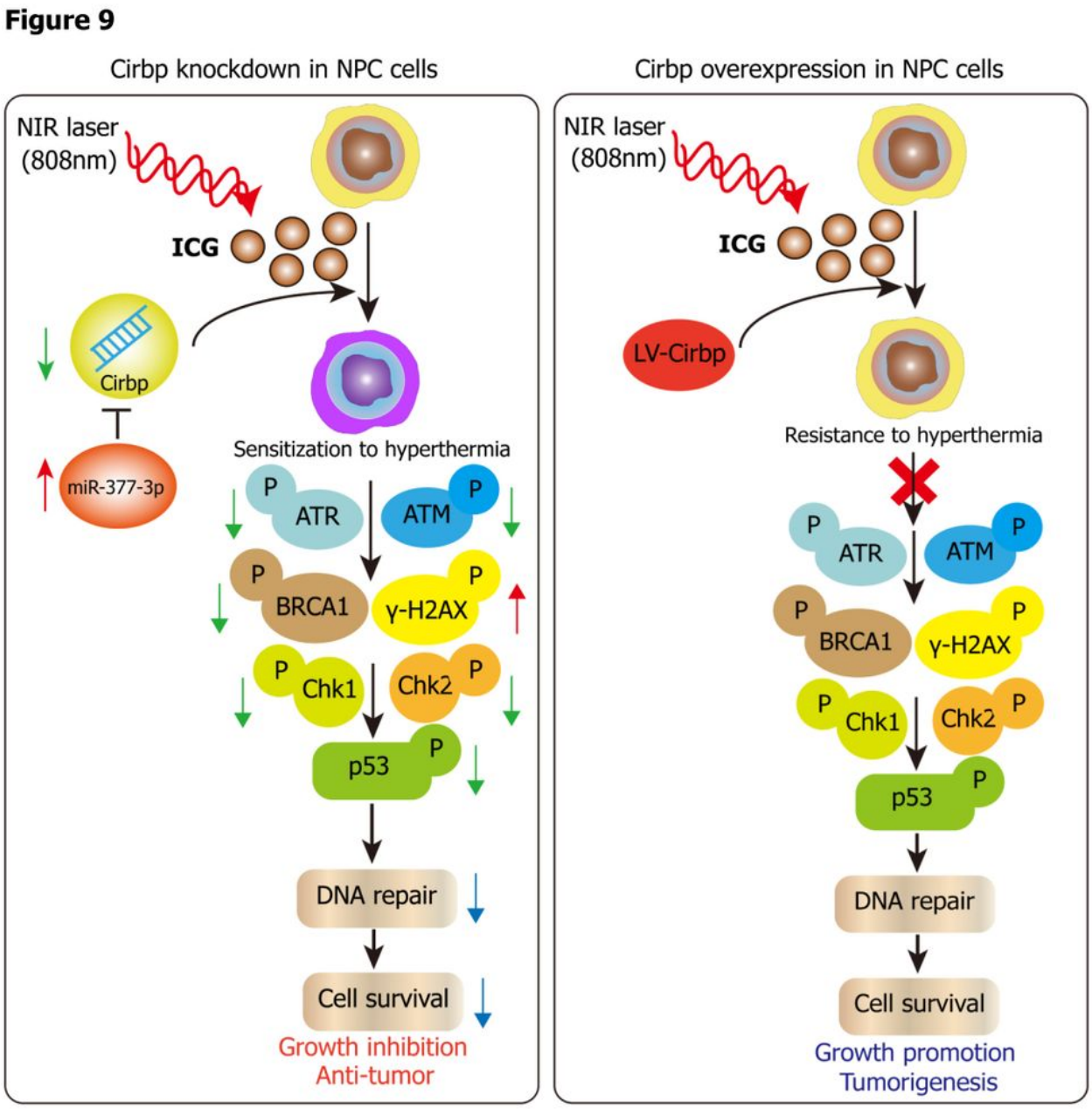

Figure 9

A proposed mechanism of Cirbp-mediated resistance and sensitization to hyperthermia.

Supplementary Files

This is a list of supplementary files associated with this preprint. Click to download.

- SupplementaryTablesTableS3toS12.xlsx
- SupplementaryTablesandFigures.pdf